

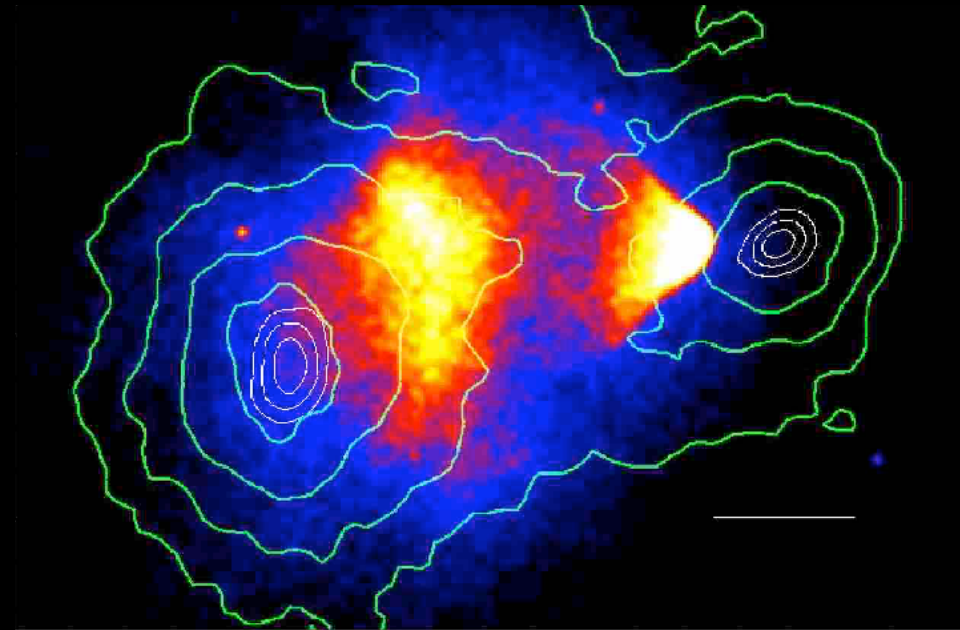
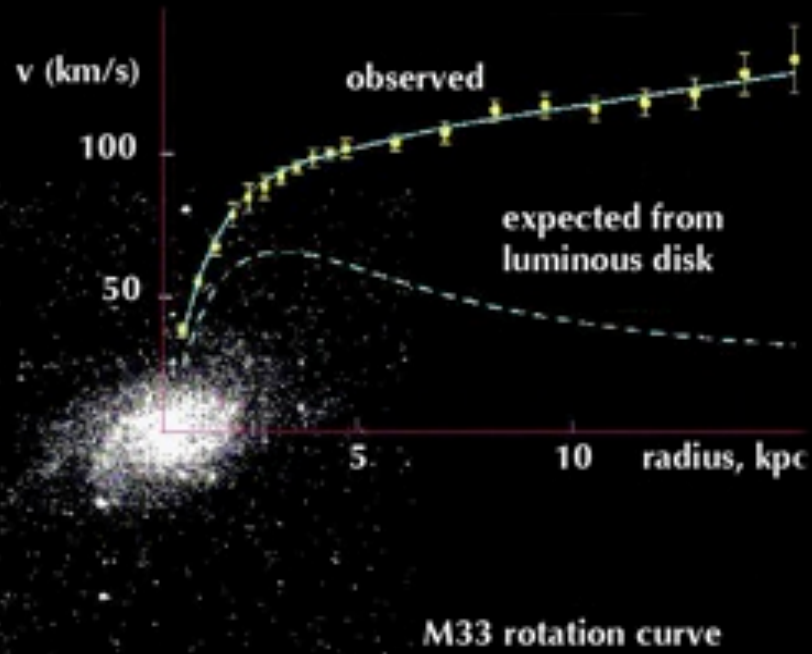
IFAE 2023

DARK MATTER DIRECT DETECTION

GIULIANA FIORILLO
UNIVERSITÀ DEGLI STUDI DI NAPOLI "FEDERICO II" & INFN

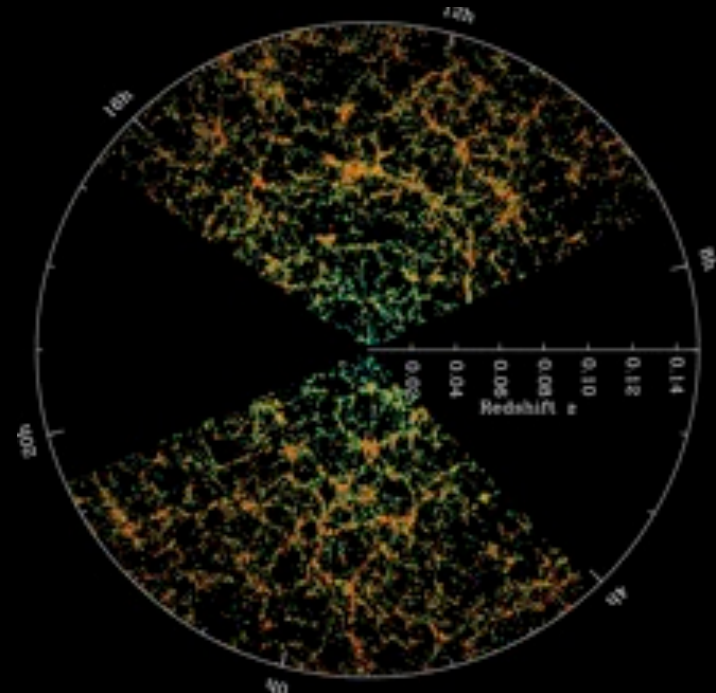
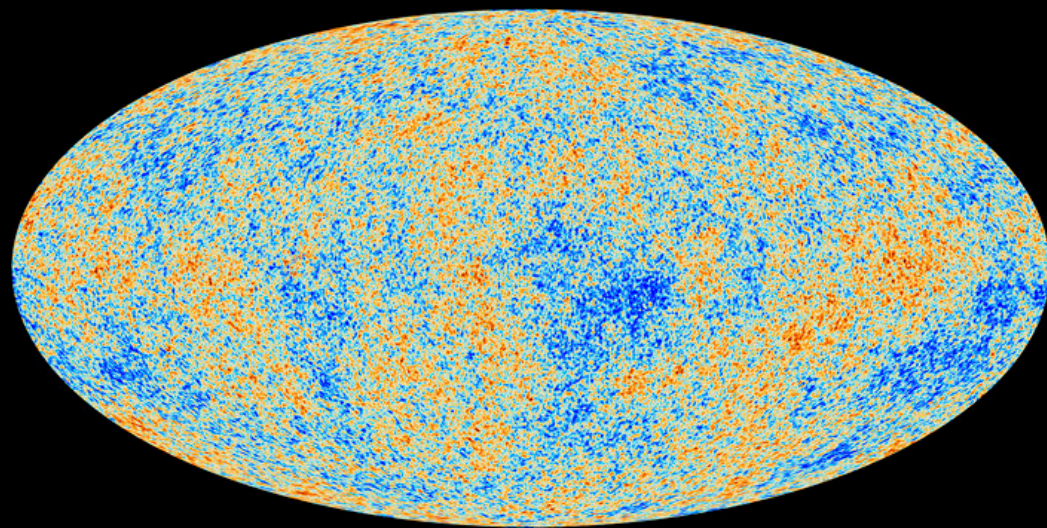
OBSERVATIONAL EVIDENCE FOR DM AT ALL SCALES

Galaxies



Galactic Clusters

CMB



Structure

A DARK UNIVERSE

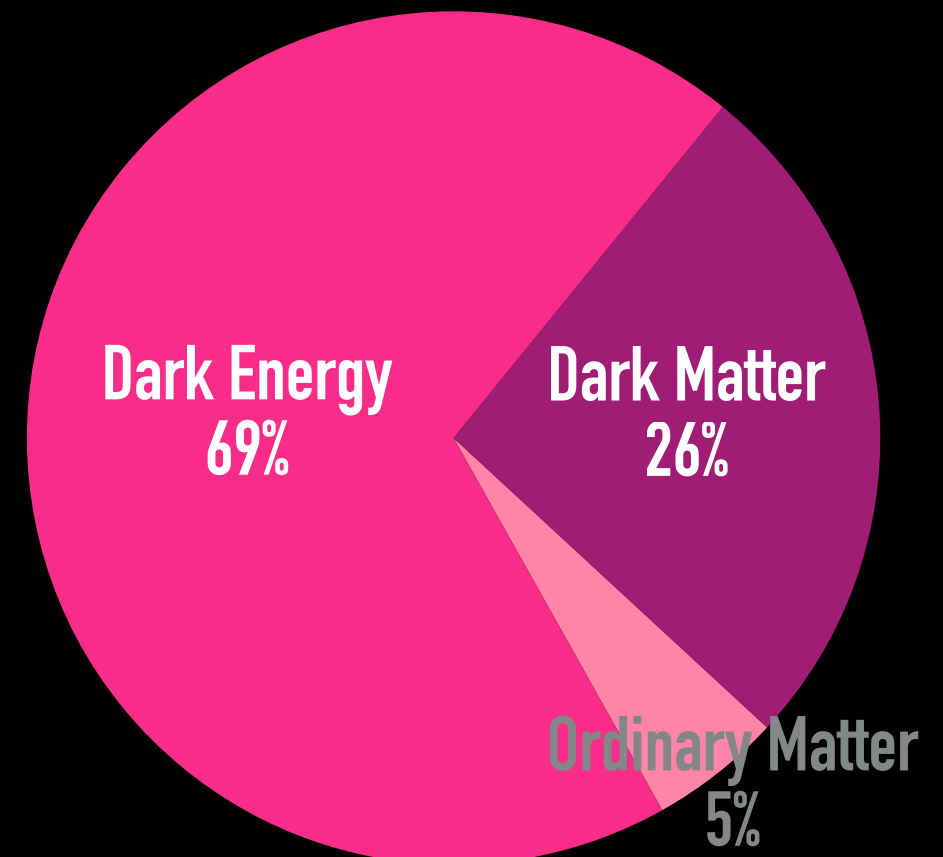
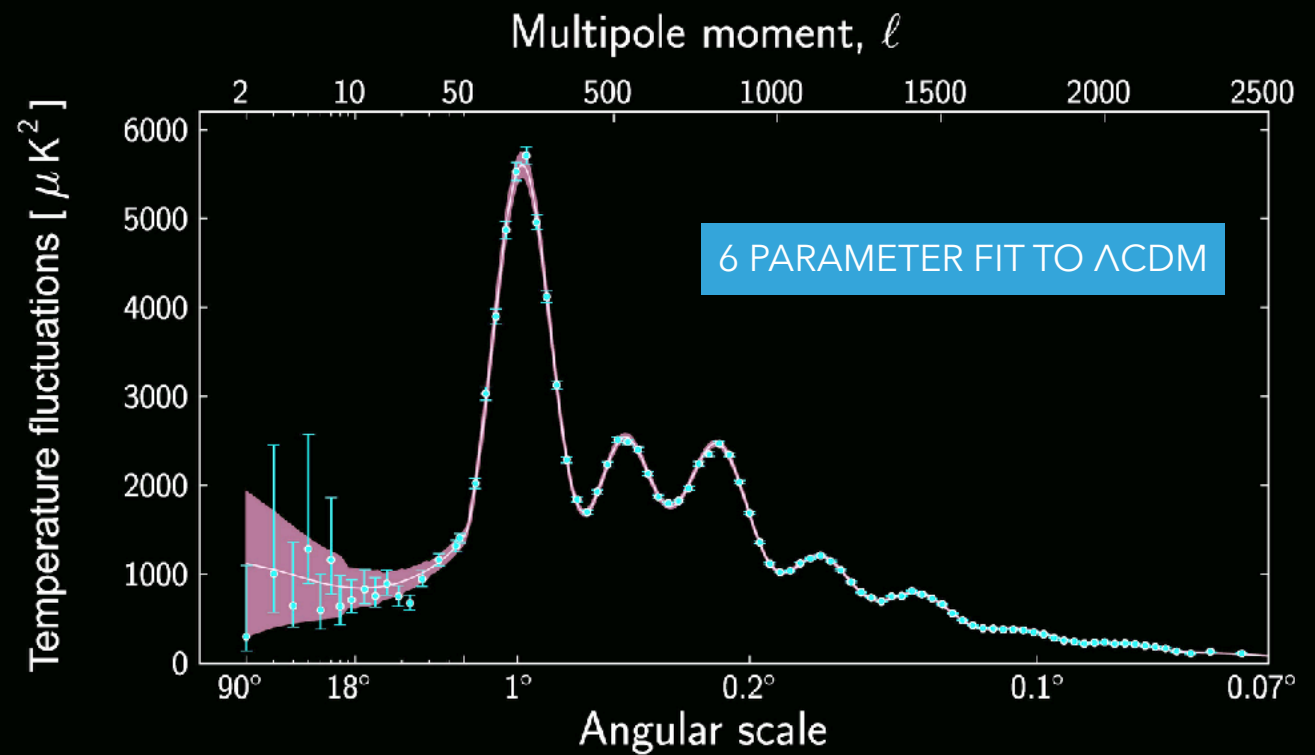
▶ Λ CDM Cosmological Model

▶ $\Omega_b h^2 = 0.02237 \pm 0.00015$

▶ $\Omega_M h^2 = 0.143 \pm 0.0011$

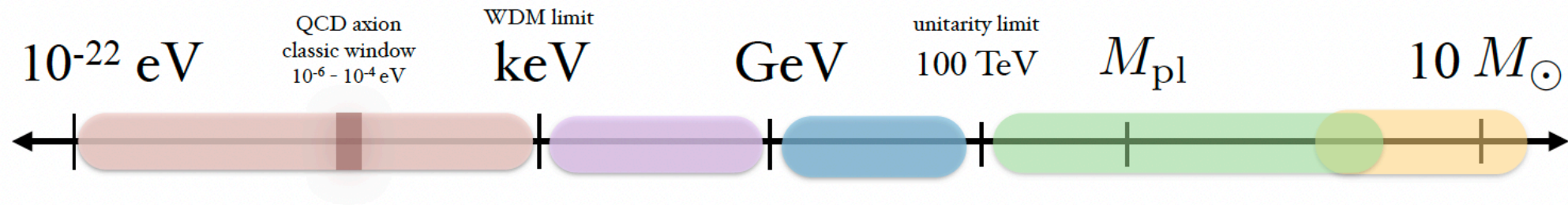
▶ 100σ difference between the baryon density and the matter density

▶ DM accounts for 85% of total matter in Universe



WHAT IS DARK MATTER?

A spectrum spanning 80 orders of magnitude



(de Broglie wavelength of galaxy)

“Ultralight” DM
non-thermal bosonic fields

“Light” DM
dark sectors
sterile ν
can be thermal

WIMP

Composite DM
(Q-balls, nuggets, etc)

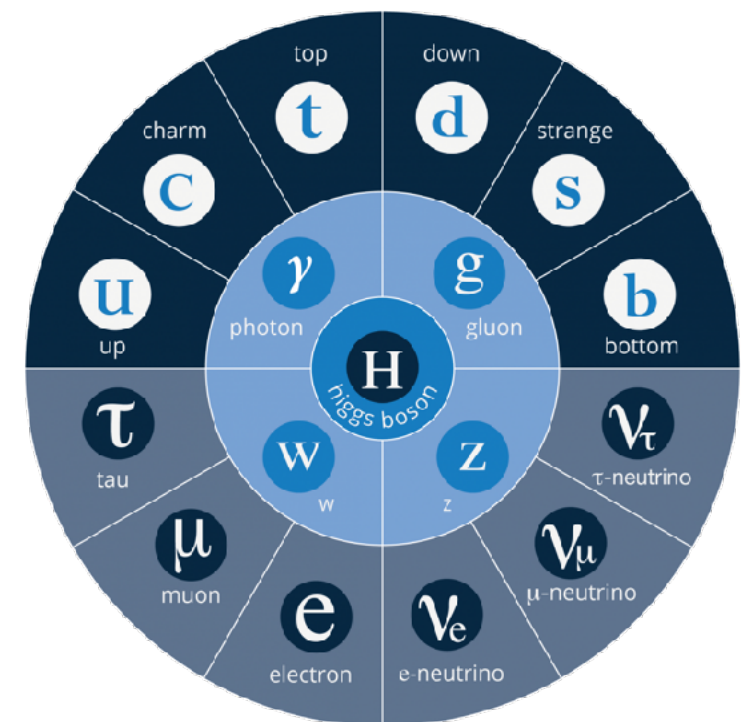
Primordial black holes

$$1 M_{\odot} = 10^{57} \text{ GeV}$$

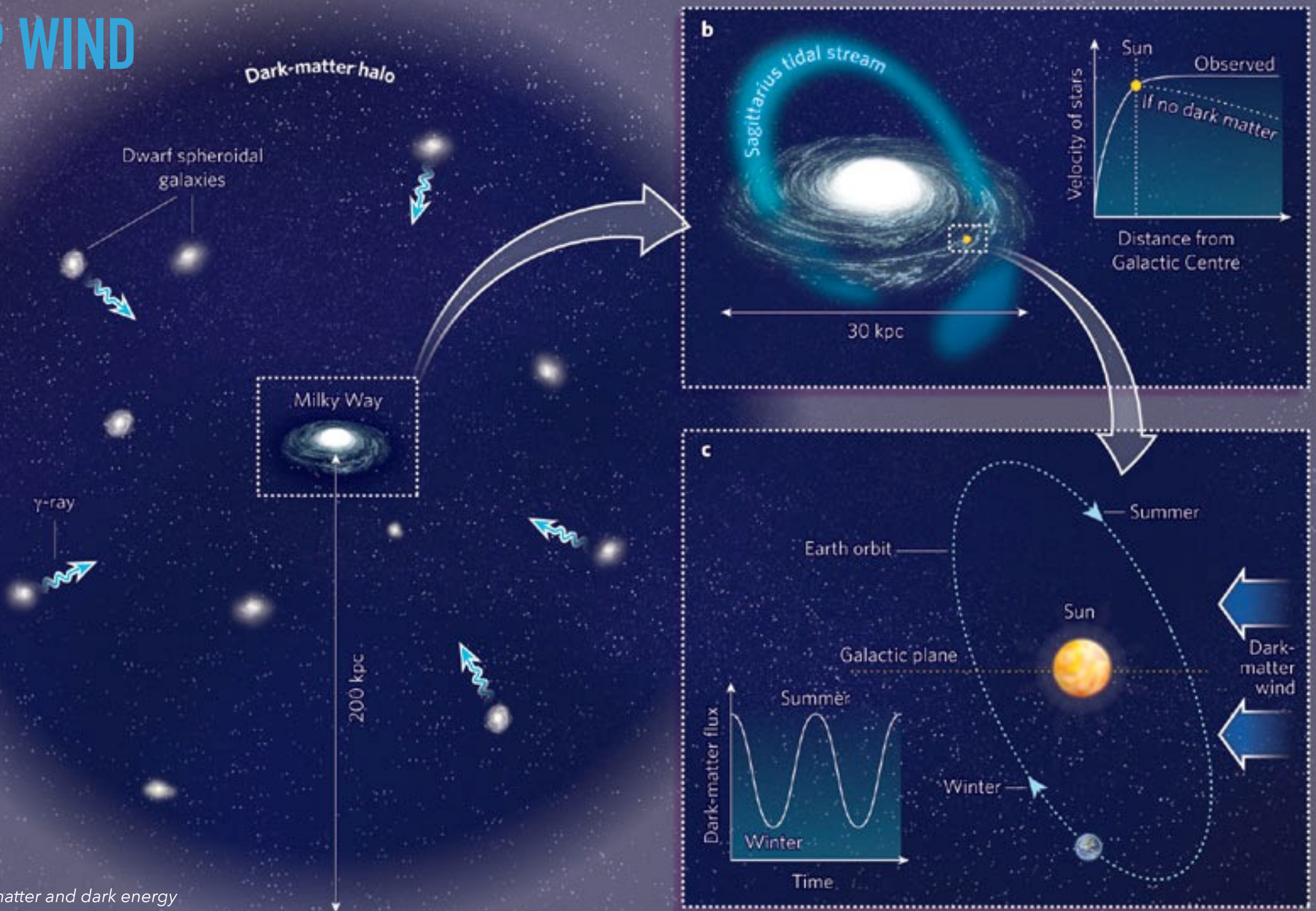
WIMP paradigm: a good place to start looking

The Minimal WIMP Model Basic Assumptions:

- Single **particle** that does not interact with itself
- Interacts weakly with Standard Model
- $2 \rightarrow 2$ annihilations primarily in s-wave
- Annihilations set thermal abundance today



WIMP WIND



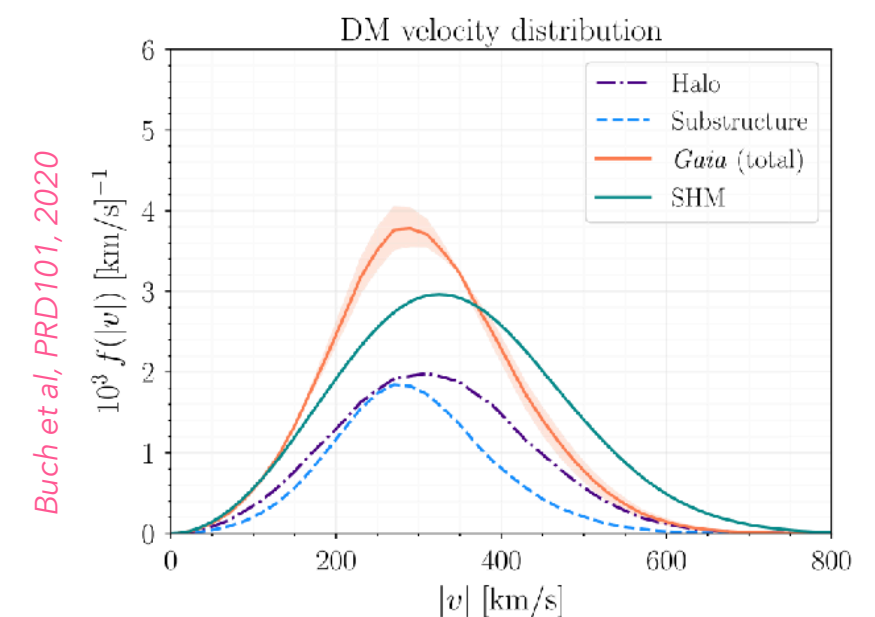
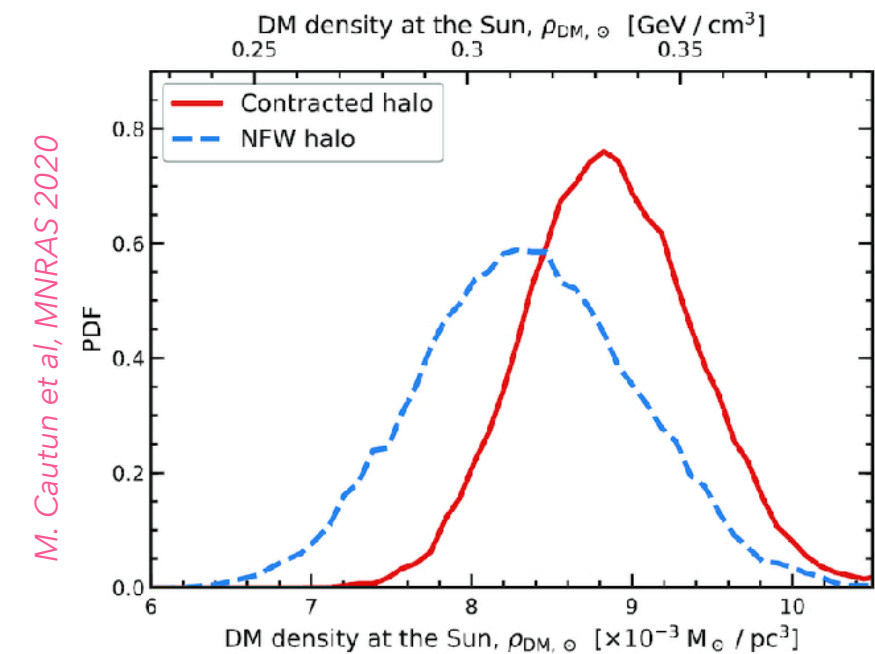
WIMP WIND ON EARTH

- ▶ Goodman & Witten (1985): "Detectability of certain dark matter candidates"

$$\frac{dR}{dE_R} = N_T \frac{\rho_\chi}{m_\chi} \times \int dv f(v) v \frac{d\sigma_\chi}{dE_R}$$

- ρ_χ galactic dark matter halo local density
- v relative velocity wrt terrestrial detector
- σ_χ elastic scattering off target nuclei

$$\Phi \simeq \frac{10^5}{\text{s cm}^2} \times \left(\frac{100 \text{ GeV}}{m_\chi} \right)$$



WIMP-NUCLEON SCATTERING

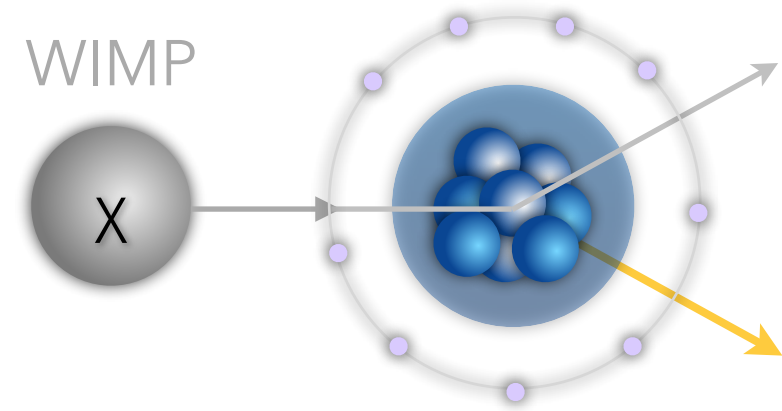
- ▶ Non-relativistic scattering
 $v/c \simeq 10^{-3}$

$$E_0 = \frac{1}{2} m_\chi v^2; \quad r = \frac{4m_\chi m_N}{(m_\chi + m_N)^2}$$

$$E_R = E_0 r \frac{(1 - \cos \theta)}{2}$$

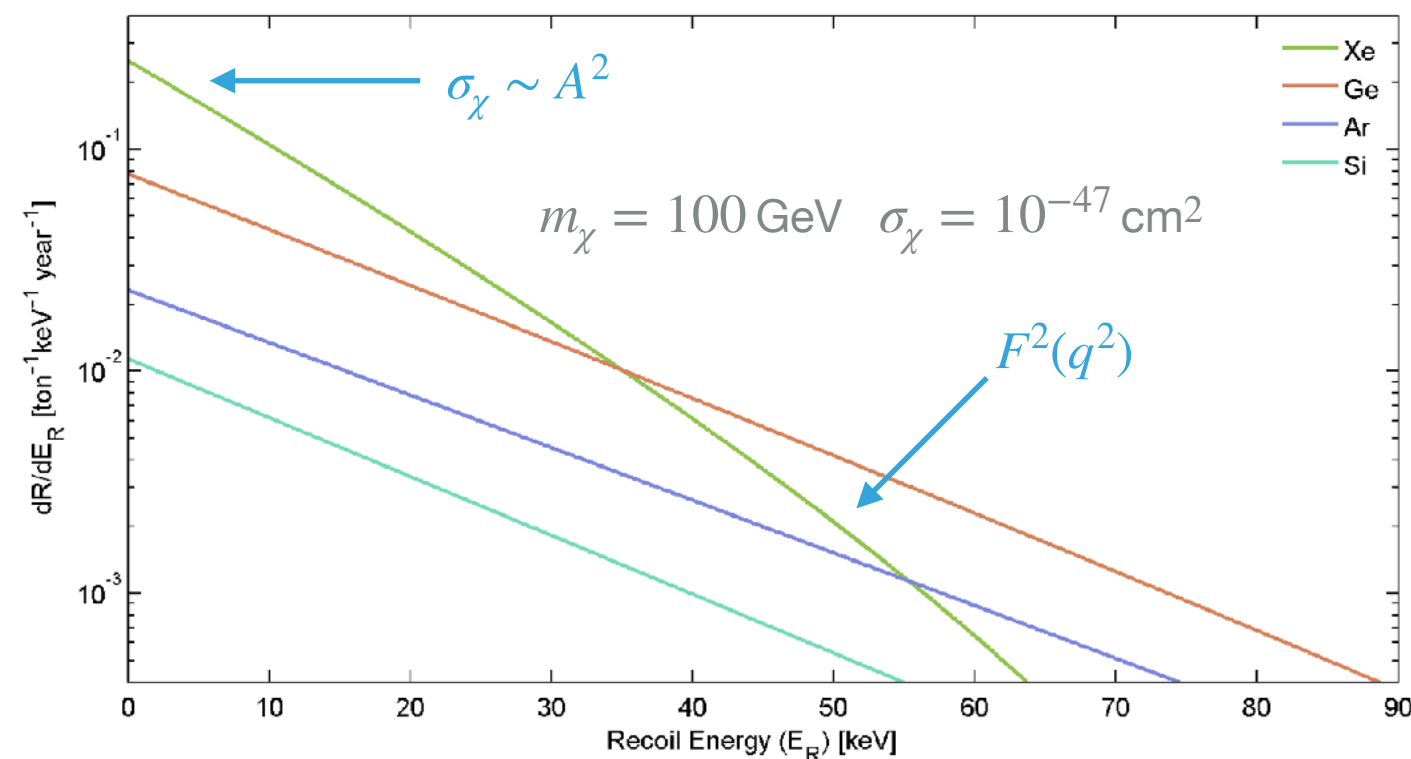
- ▶ Contact interaction independent of momentum exchange (nucleus as a particle, with charge and spin)

- ➔ standard SI/SD description
- ➔ nuclear form factors generally included



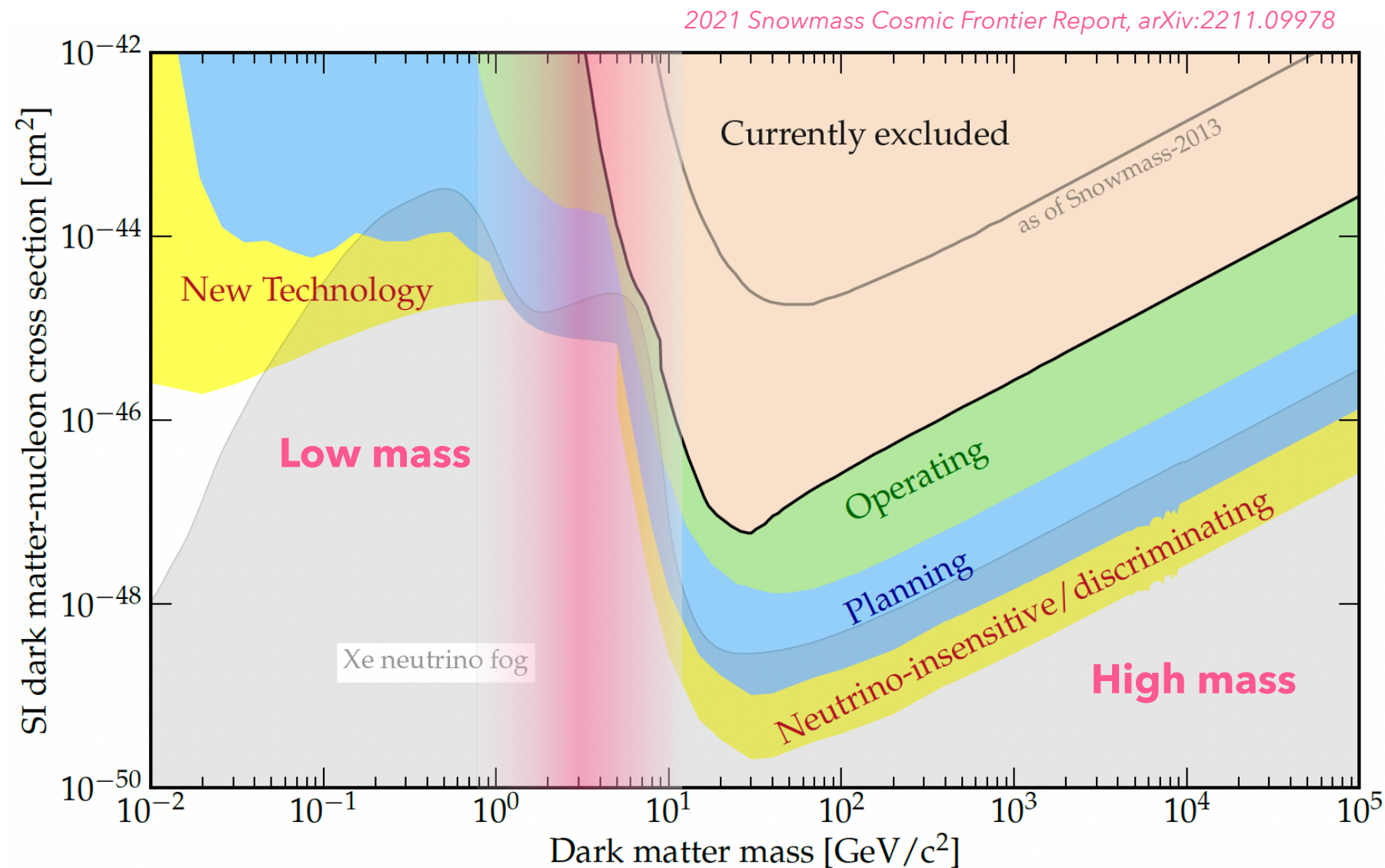
$$\frac{dR}{dE_R} = \frac{R_0}{E_0 r} \exp\left(-\frac{E_R}{E_0 r}\right) \times [S(E_R) F^2(q^2) I]$$

$F^2(q^2)$ Form factor
 $S(E_R)$ seasonal modulation
 I Interaction type

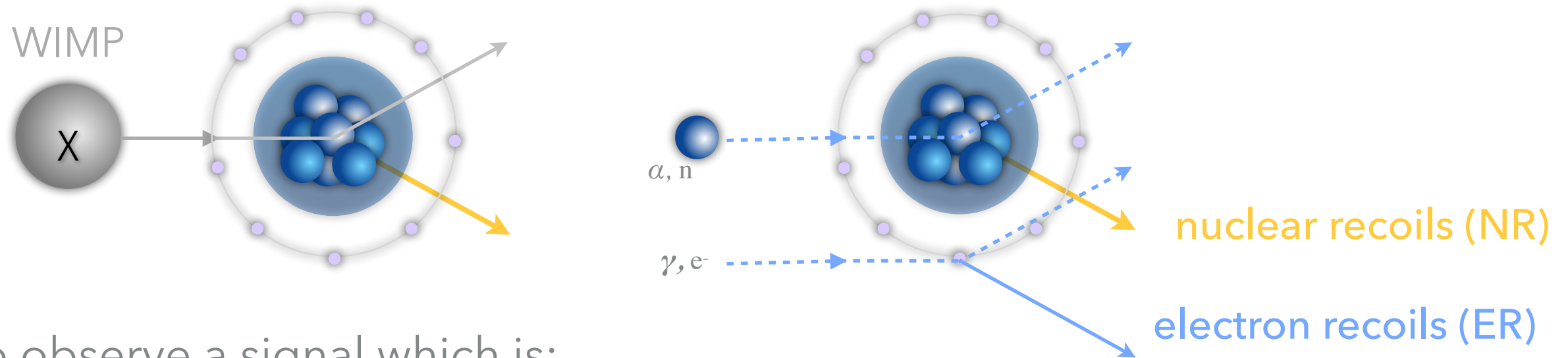


WIMP NUCLEON SI INTERACTION EXCLUSION LIMITS LANDSCAPE

- ▶ To improve sensitivity:
 - larger exposure $M \times T$ and lower background
- ▶ To extend sensitivity at low mass WIMPs:
 - lower energy threshold
- ▶ Minimum of the curve:
 - depends on target nuclei

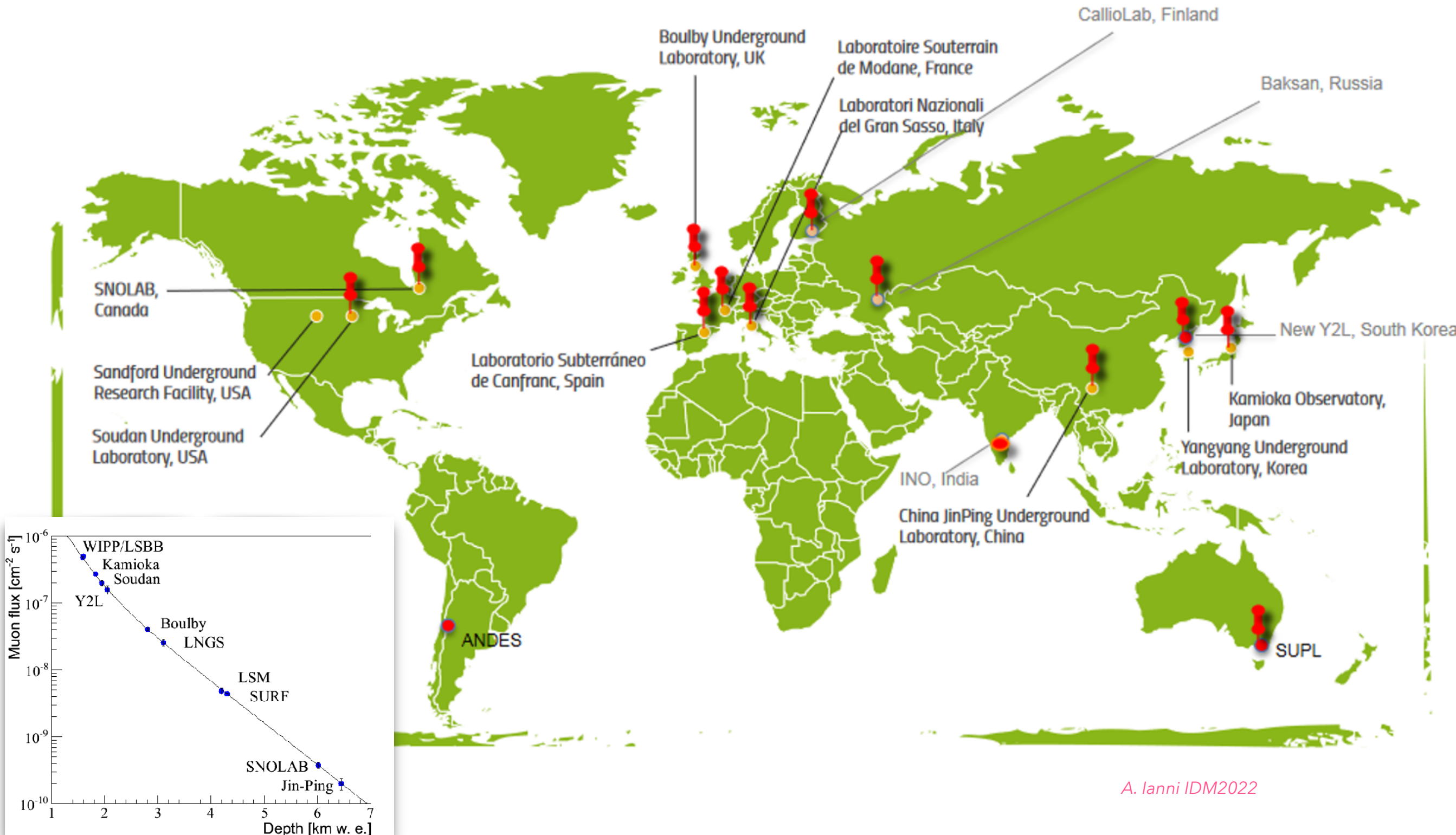


EXPERIMENTAL CHALLENGE

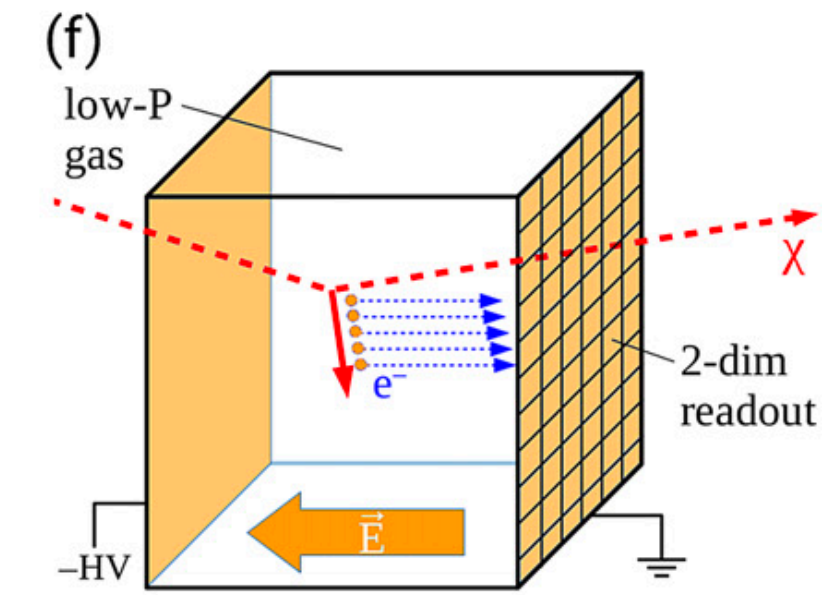
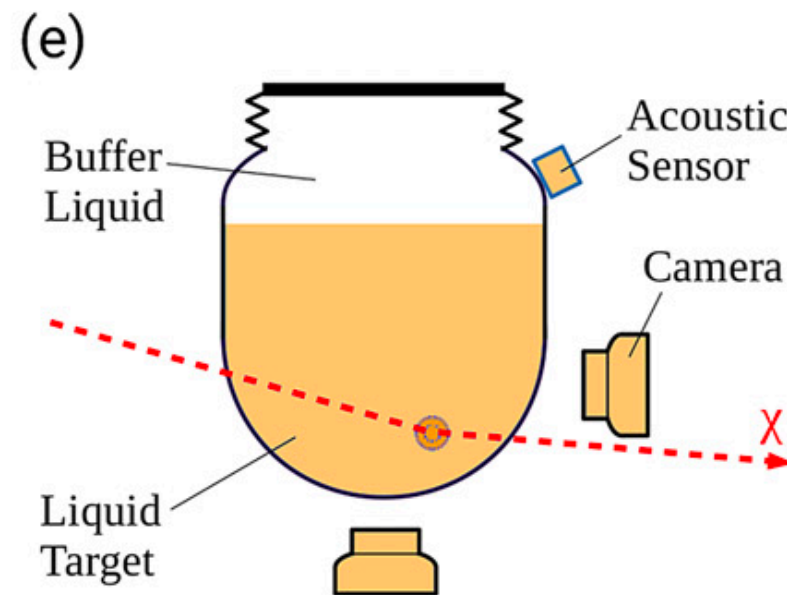
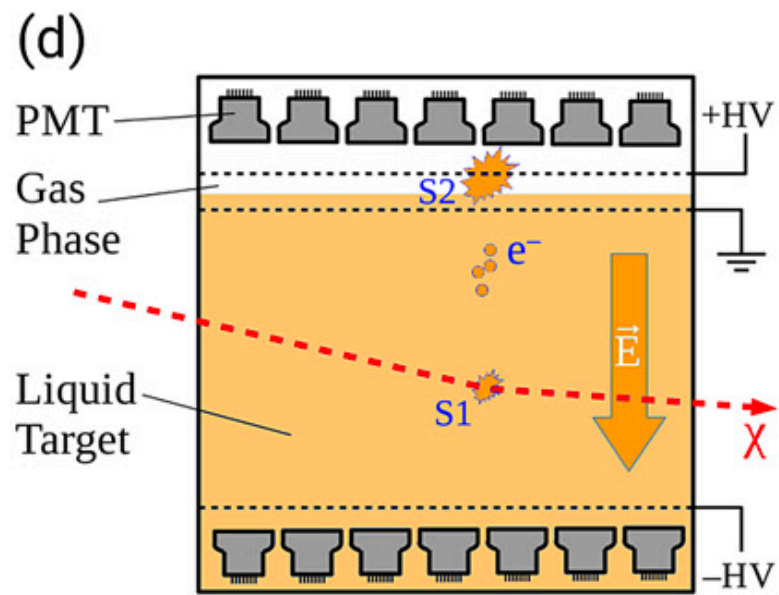
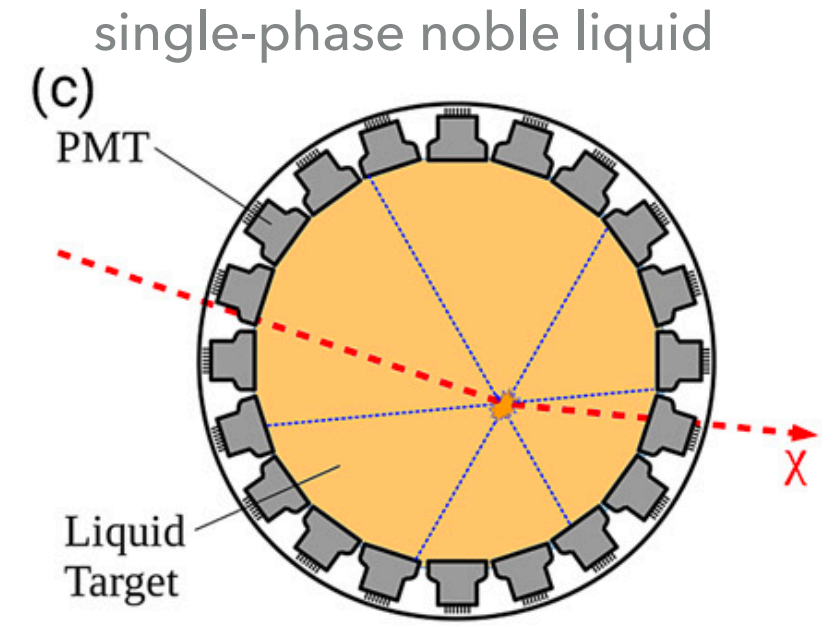
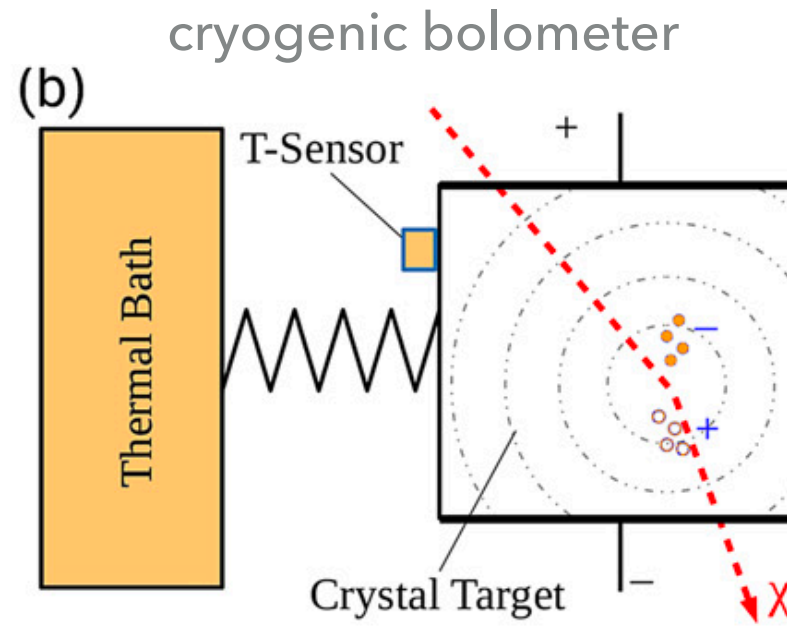
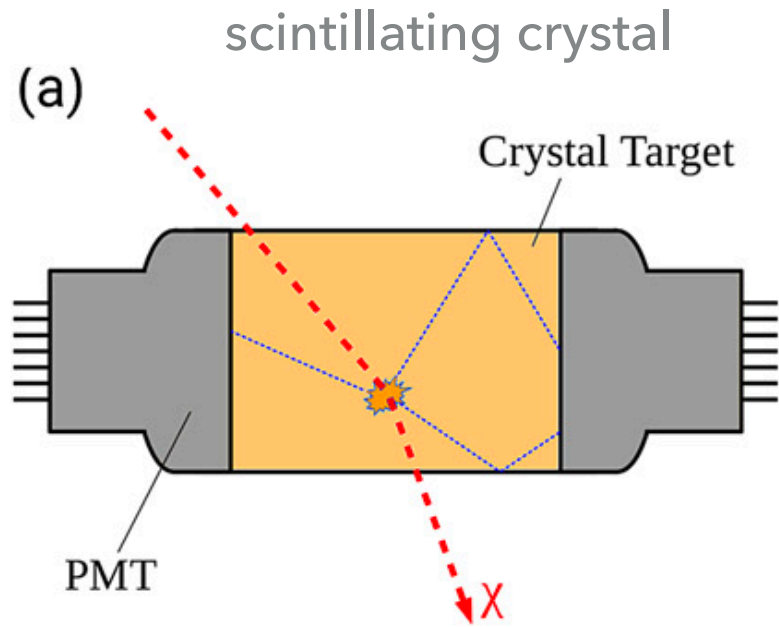


- ▶ To observe a signal which is:
 - very small: **low recoil energies < 100 keV**
 - very rare: **< 1 event/(kg y) at low masses and < 1 event/(t y) at high masses**
 - buried in backgrounds with $> 10^6$ higher rates:
 - Muon-induced neutrons: **NRs**
 - Cosmogenic activation of materials/targets: **ERs**
 - Radioactivity of detector materials: **NRs** and **ERs**
 - Target intrinsic isotopes: **ERs**

DEEP UNDERGROUND LABORATORIES



DETECTOR TECHNOLOGIES



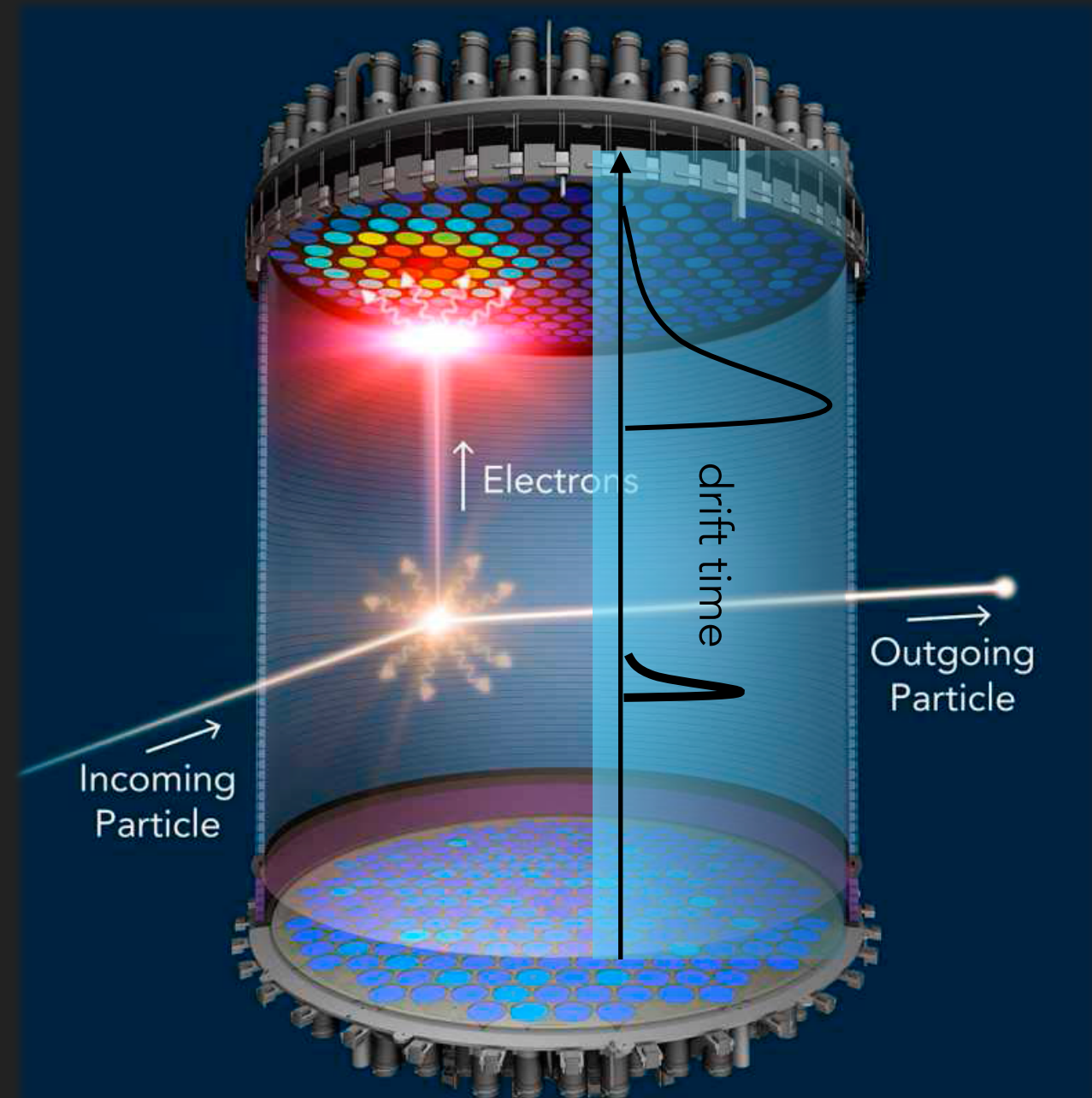
dual-phase noble liquid TPC

bubble chamber

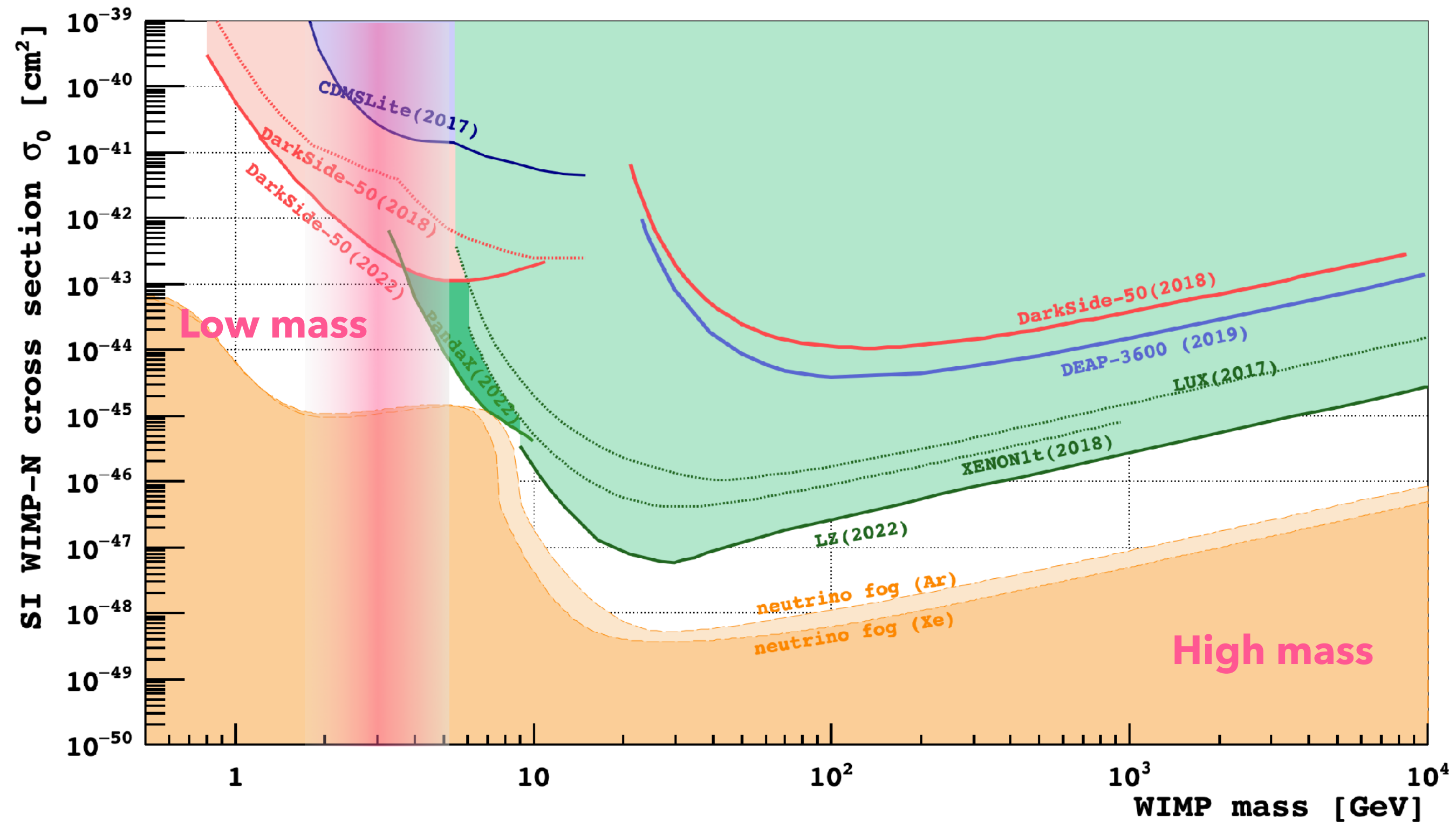
directional detector

LARGE EXPOSURE: NOBLE LIQUID TPC

- ▶ dual-phase Time Projection Chambers with multi-tonne liquid Xe, Ar targets
- ▶ read out primary scintillation: "S1" + proportional gas scintillation from drifted electrons: "S2"
- ▶ 3D position reconstruction:
 - ▶ time difference between S1 and S2 gives Z position (few mm resolution)
 - ▶ pattern of S2 light gives XY position (~1cm resolution)
- ▶ background identification + passive suppression
- ▶ zeptobarn (10^{-45} cm^2) to yoctobarn (10^{-48} cm^2) sensitivity to WIMP dark matter

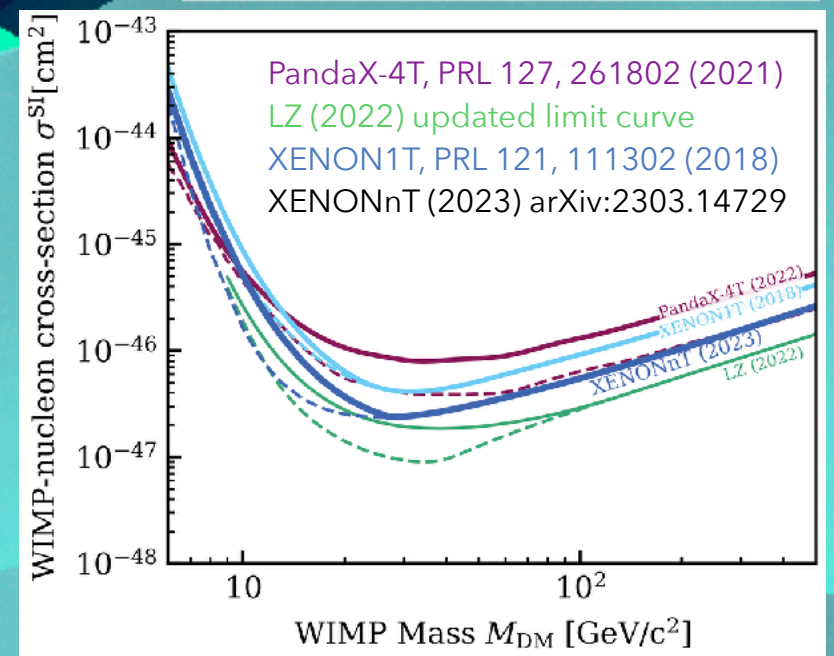
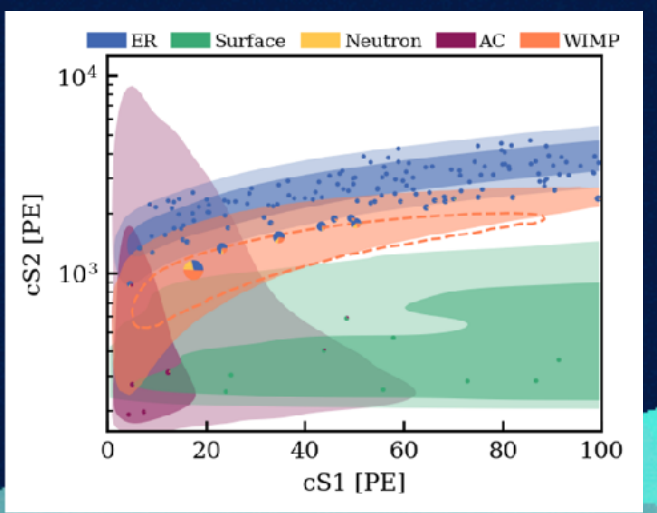
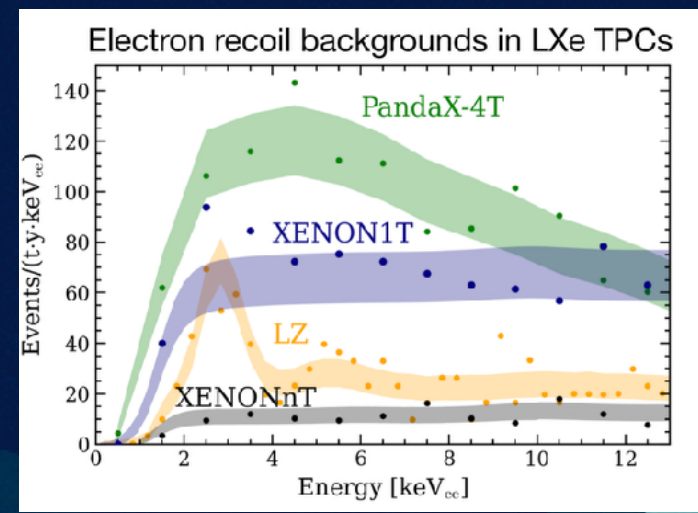
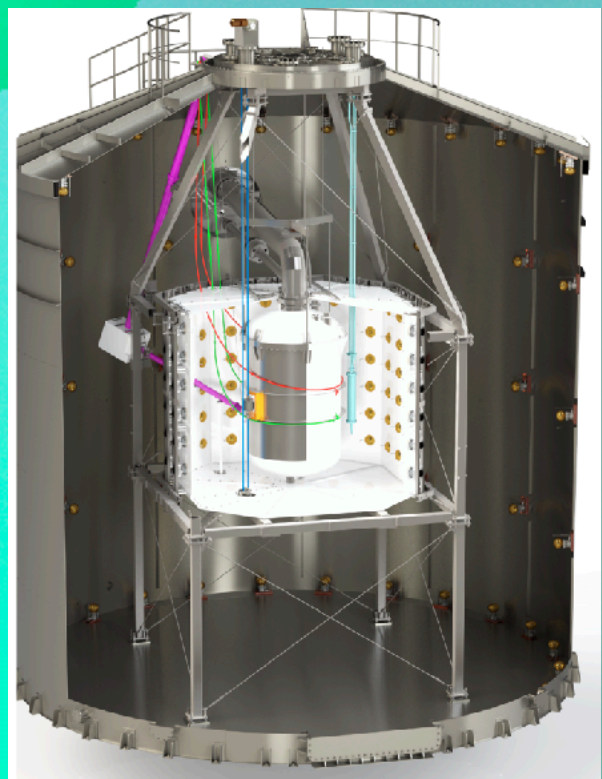
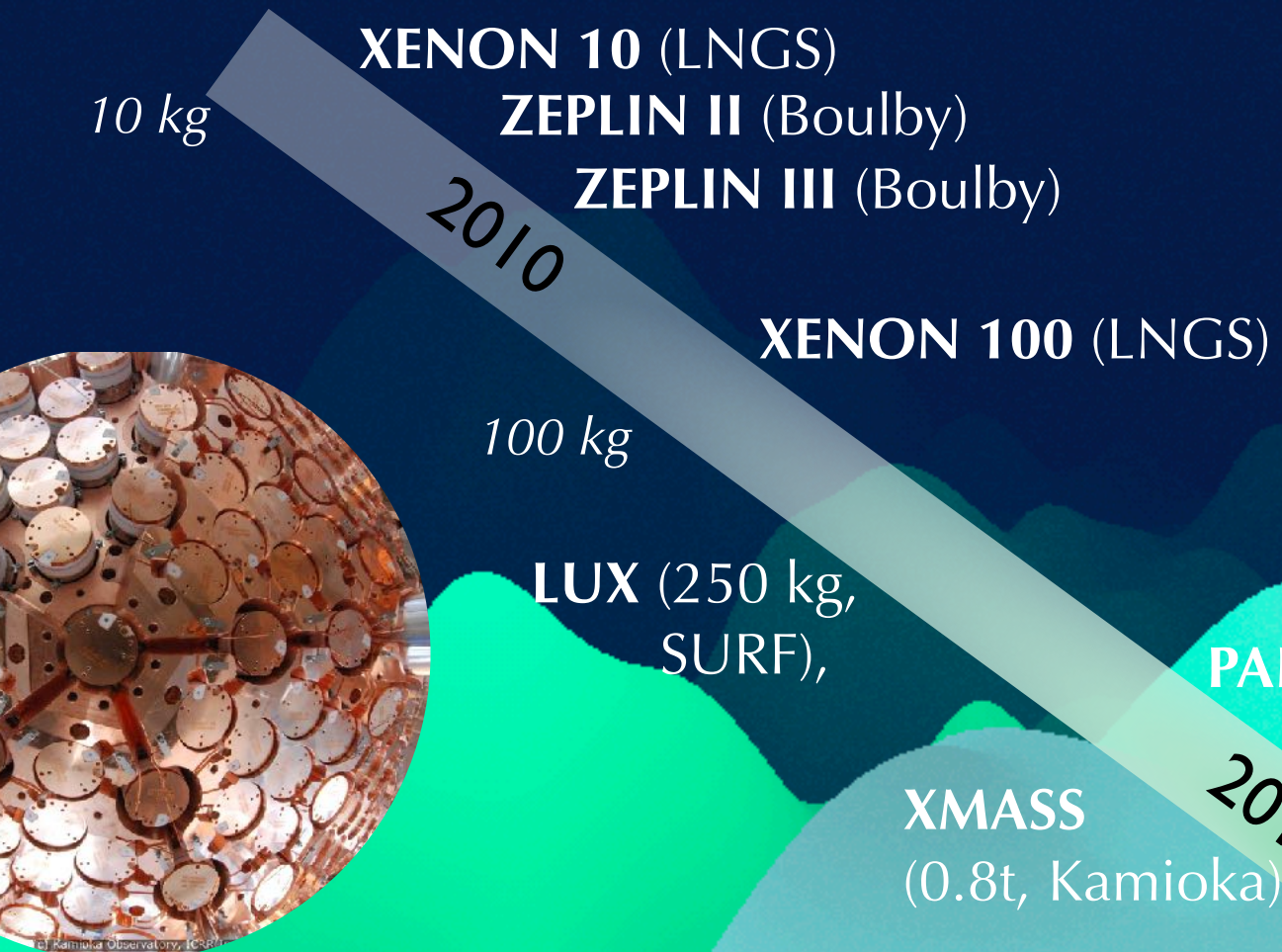


SENSITIVE TO A BROAD RANGE OF WIMP MASSES



XENON DETECTORS

LZ: best limit for high WIMP masses
 XENON: lowest background from ER



XENON:2303.14729
 E. Aprile UCLA DM2023

XLZD Consortium formed

arXiv:2203.02309v1

ARGON DETECTORS

LAr high mass: background discrimination

10 kg
2010

DarkSide-50
(50 kg, LNGS)

100 kg

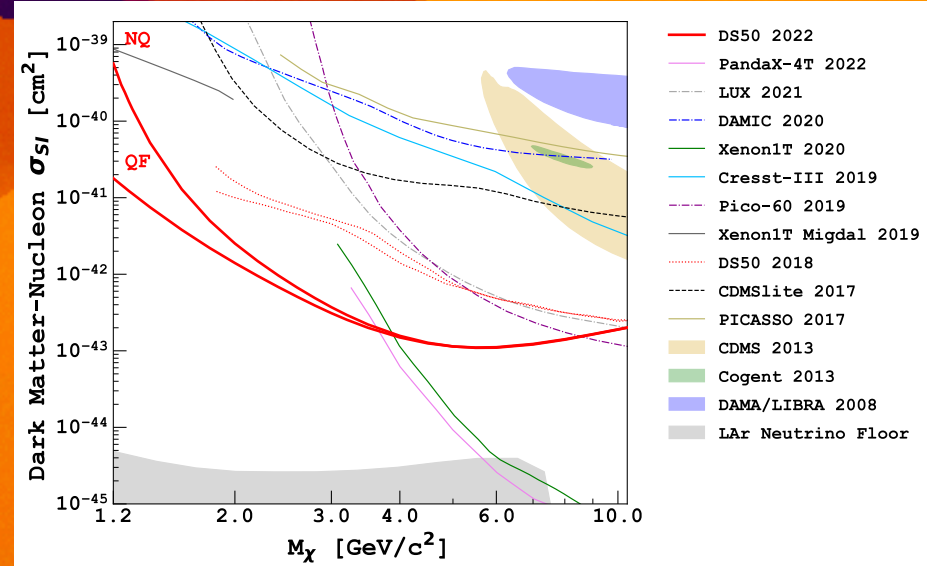
ArDM
(1t, LSC)

1000 kg

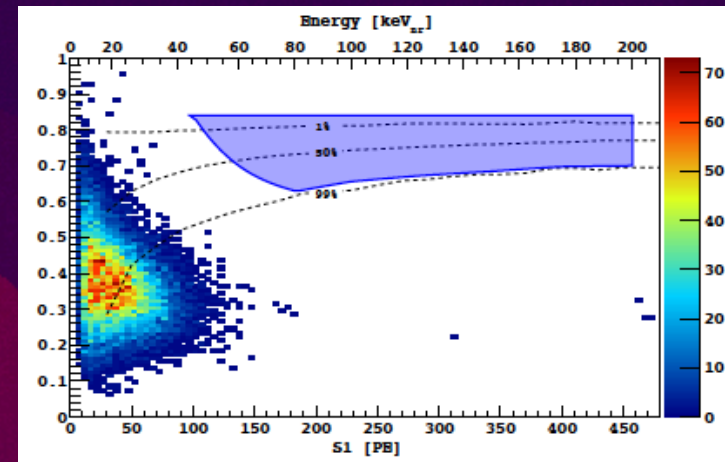
DEAP-3600
(3.6t, SNOLAB)

10000 kg

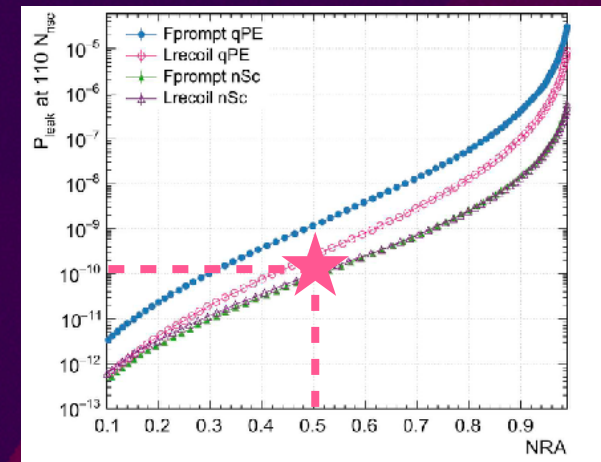
DS50 low mass:
leading SI limit at
1.2-3.6 GeV/c²



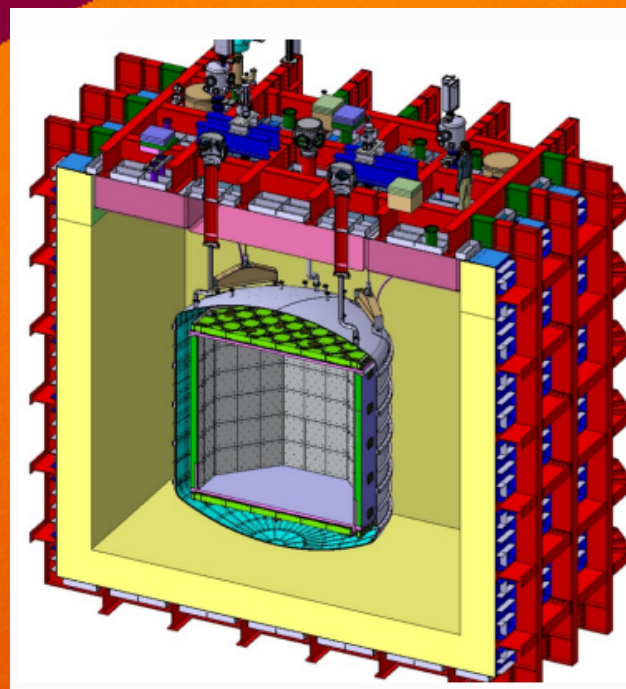
Phys. Rev. D 107, 063001 (2023)



Phys. Rev. D 98, 102006 (2018)



Eur. Phys. J. C 81, 823 (2021)



*Global Argon
Dark Matter
Collaboration
formed*

2020

DarkSide-20k
(50t, LNGS)

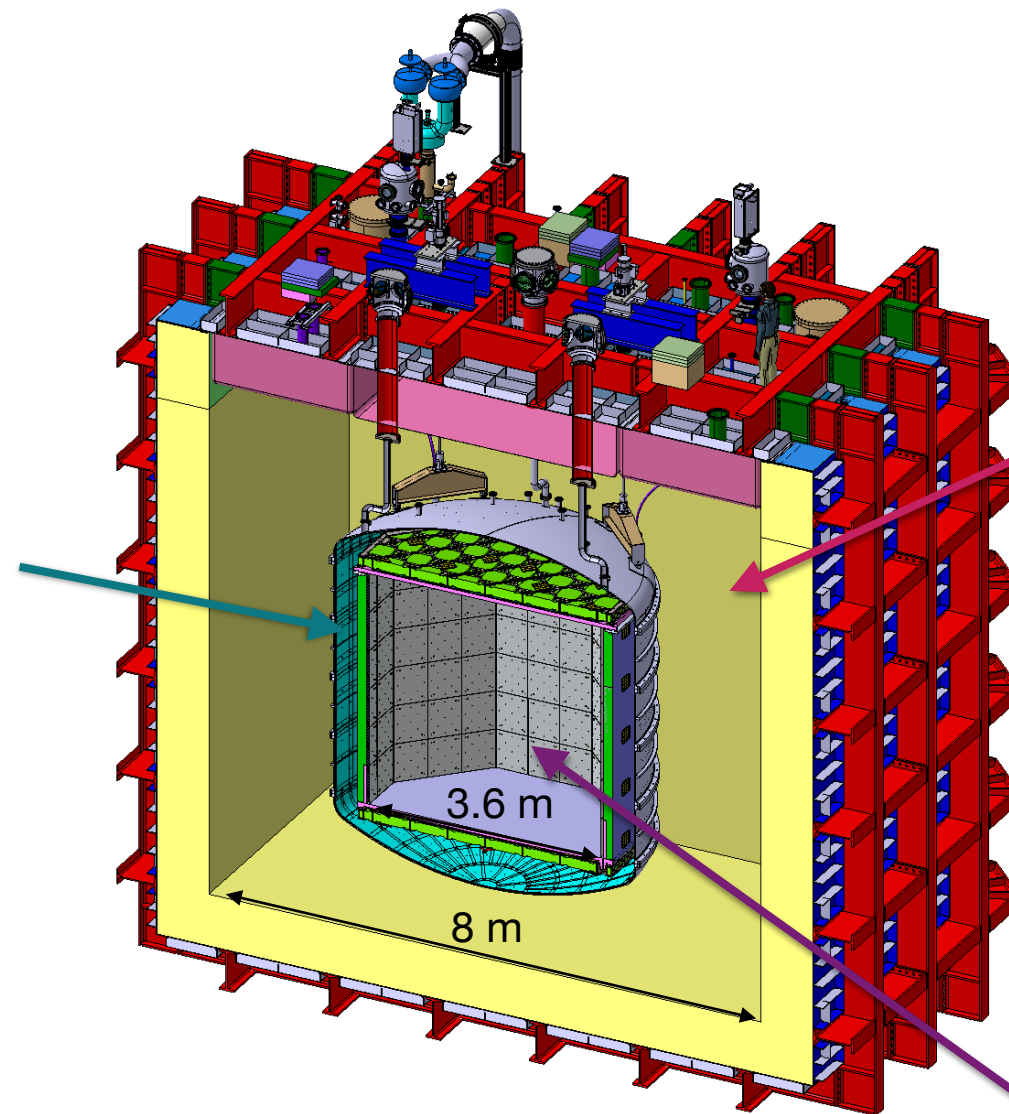
100000 kg

ARGO: 400 t, SNOLAB

THE DARKSIDE-20K DETECTOR

Inner Veto

Radiogenic n 's
12-ton underground
LAr



Outer Veto

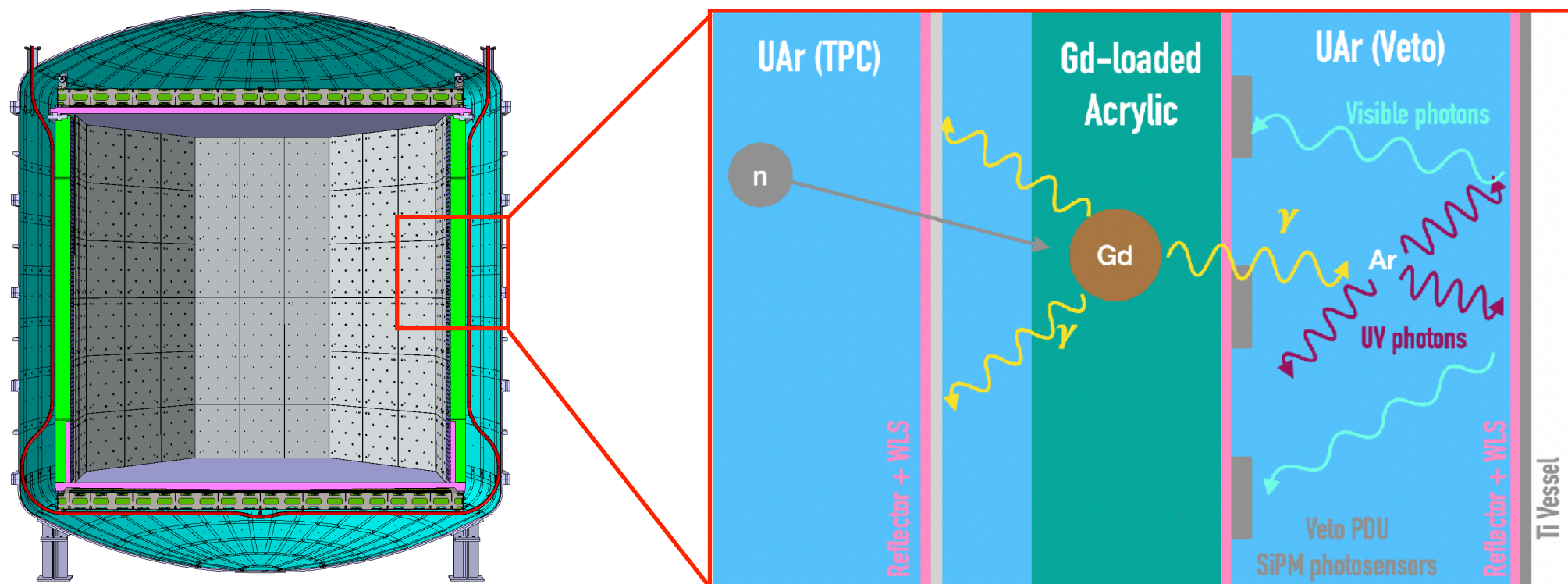
Cosmic μ 's and showers
600-ton atmospheric LAr

TPC

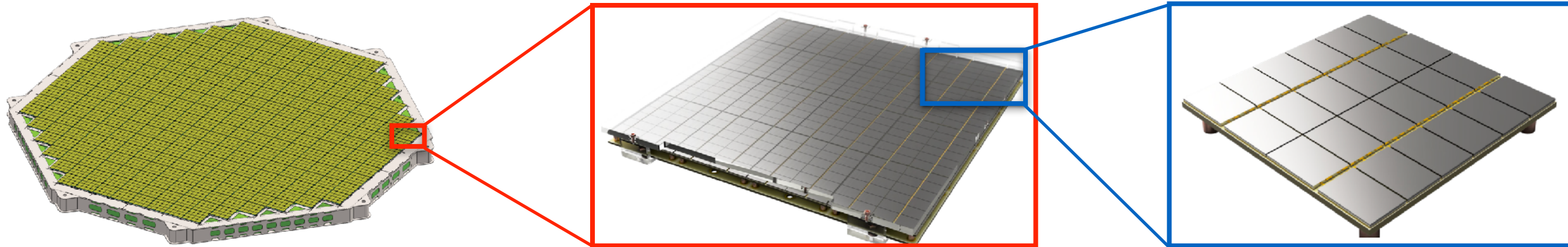
Dark matter detector
50-ton underground LAr/GAr
(20-ton fiducial mass)

NEUTRON TAGGING VIA Gd-LOADED ACRYLIC

- ▶ γ -rays ($<8\text{MeV}$) from n capture by Gd
- ▶ n -tagging efficiency $\sim 90\%$
- ▶ R&D finished and production started



LOW RADIOACTIVITY, HIGH EFFICIENCY SiPM PHOTODENSORS

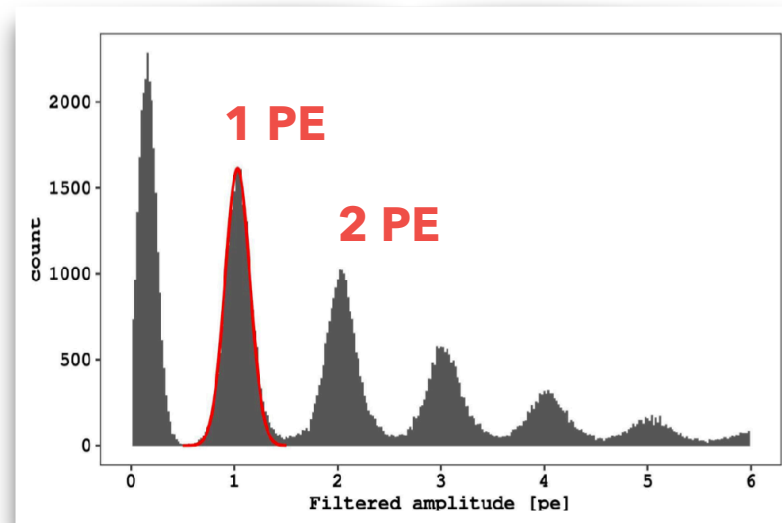


TPC optical plane ($\sim 21 \text{ m}^2$)
525 PDUs

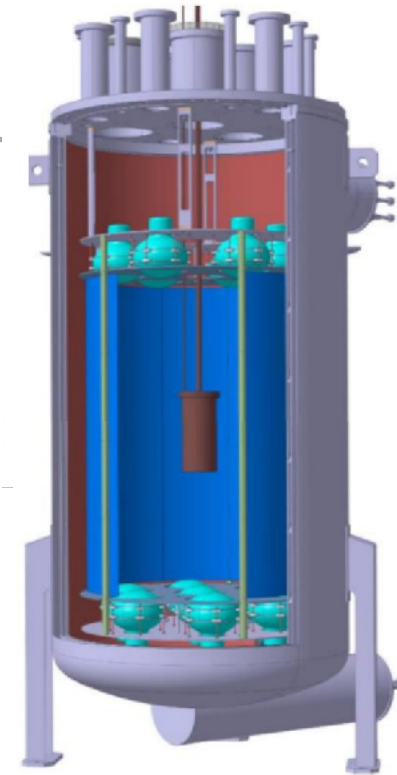
Photo Detection Unit
16 tiles arranged into 4 channels

Tile / photo-detector module
24 SiPMs + signal amplifier

- ▶ Wafer delivery from LFoundry started in 2022
- ▶ Packaging and assembly for TPC sensors: **Nuova Officina Assergi** (NOA), about to start operations
- ▶ Packaging and assembly for Veto sensors: RAL and Liverpool, UK
- ▶ Several test facilities to qualify production: Naples, Liverpool, Edinburgh, AstroCent



LOW RADIOACTIVITY ARGON: URANIA & ARIA



1) UAr extraction at the URANIA plant.

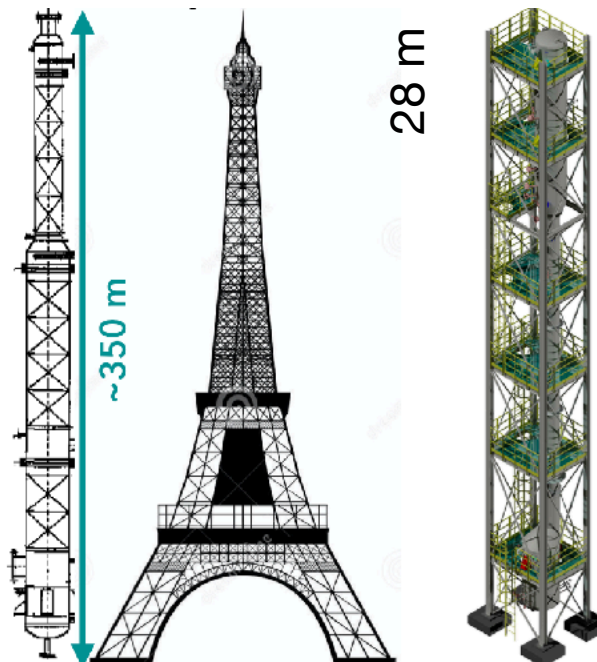
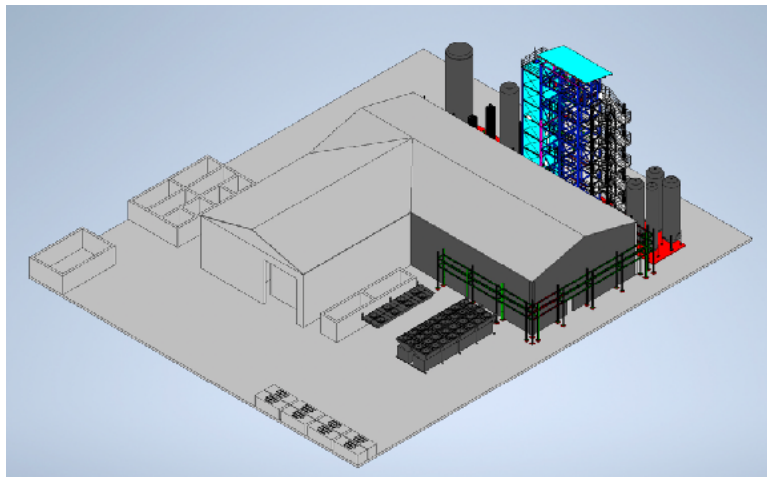
^{39}Ar (β -decay) suppressed by $\sim 10^3$ in underground CO2 reservoir in Cortez, Colorado

UAr extraction rate: 250-330 kg/day

Expected argon purity at outlet: 99.99%

3) Qualification at Canfranc, DArT in ArDM

A single-phase LAr detector with active volume $\sim 1\text{L}$, capable of measuring UAr to AAr ^{39}Ar depletion factors of the order of 1000 with 10% precision in weeks



2) Cryogenic distillation at the ARIA facility

Installed in the shaft of a coal mine

Chemical purification rate: 1 t/day

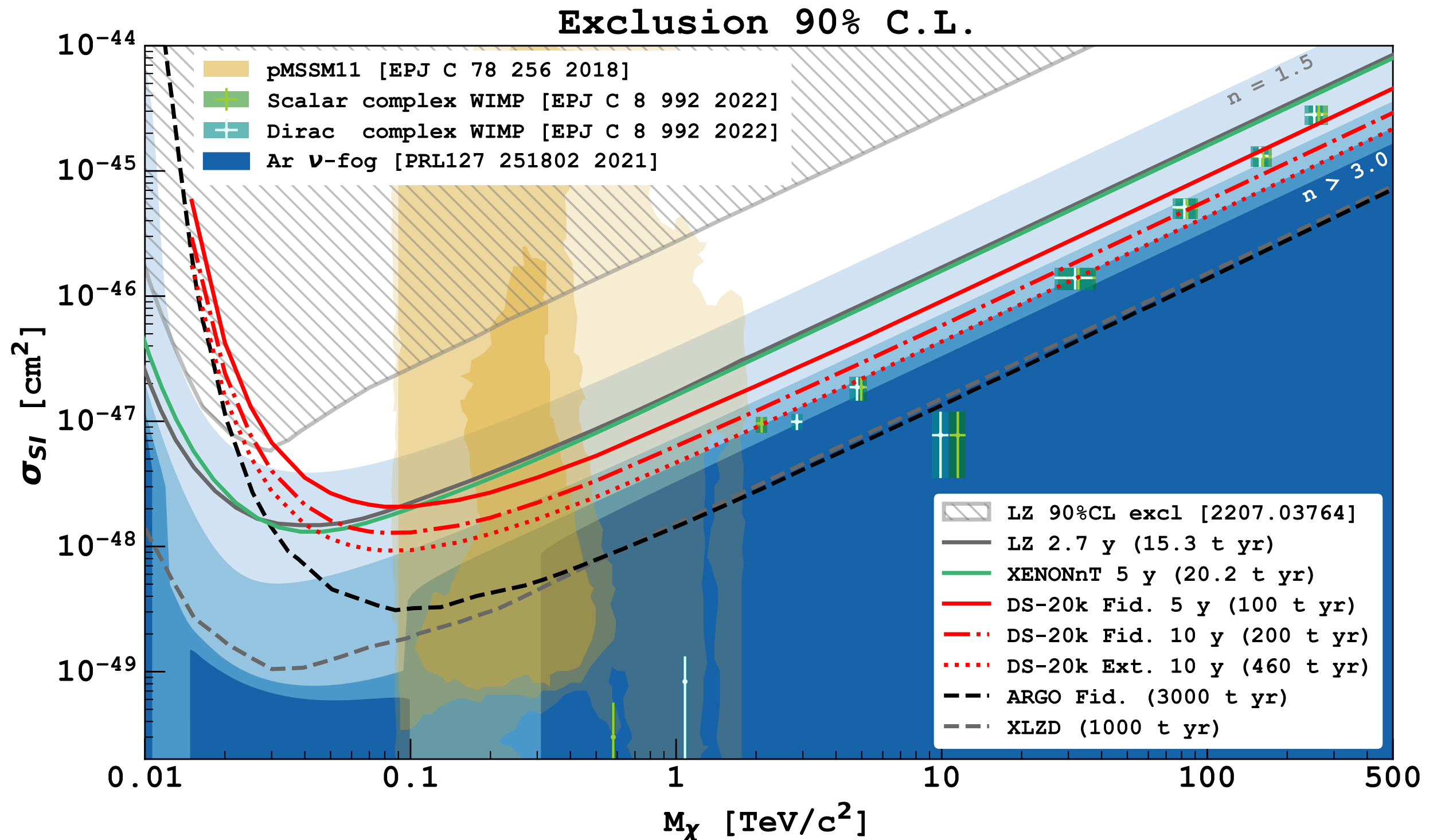
First module operated according to specs with nitrogen

Run completed with Ar at the end of 2020: results to be published soon

Full assembly about to start

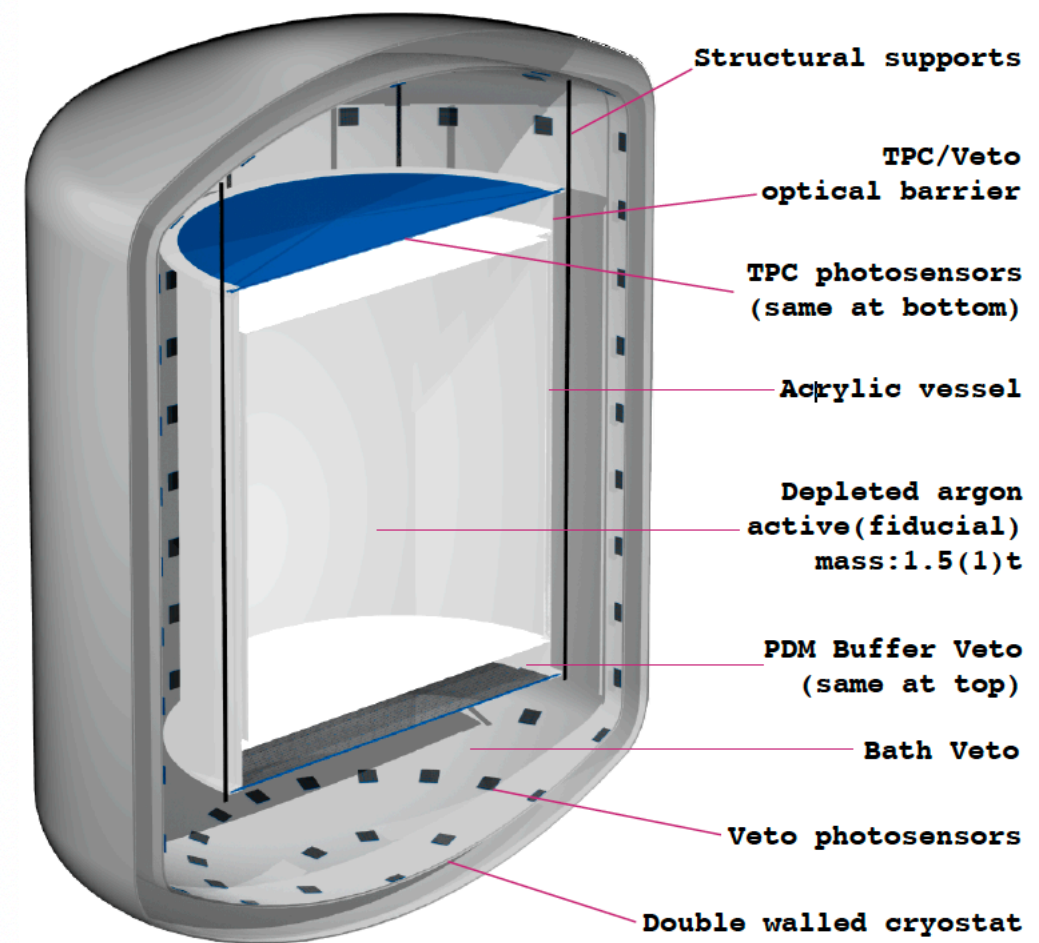
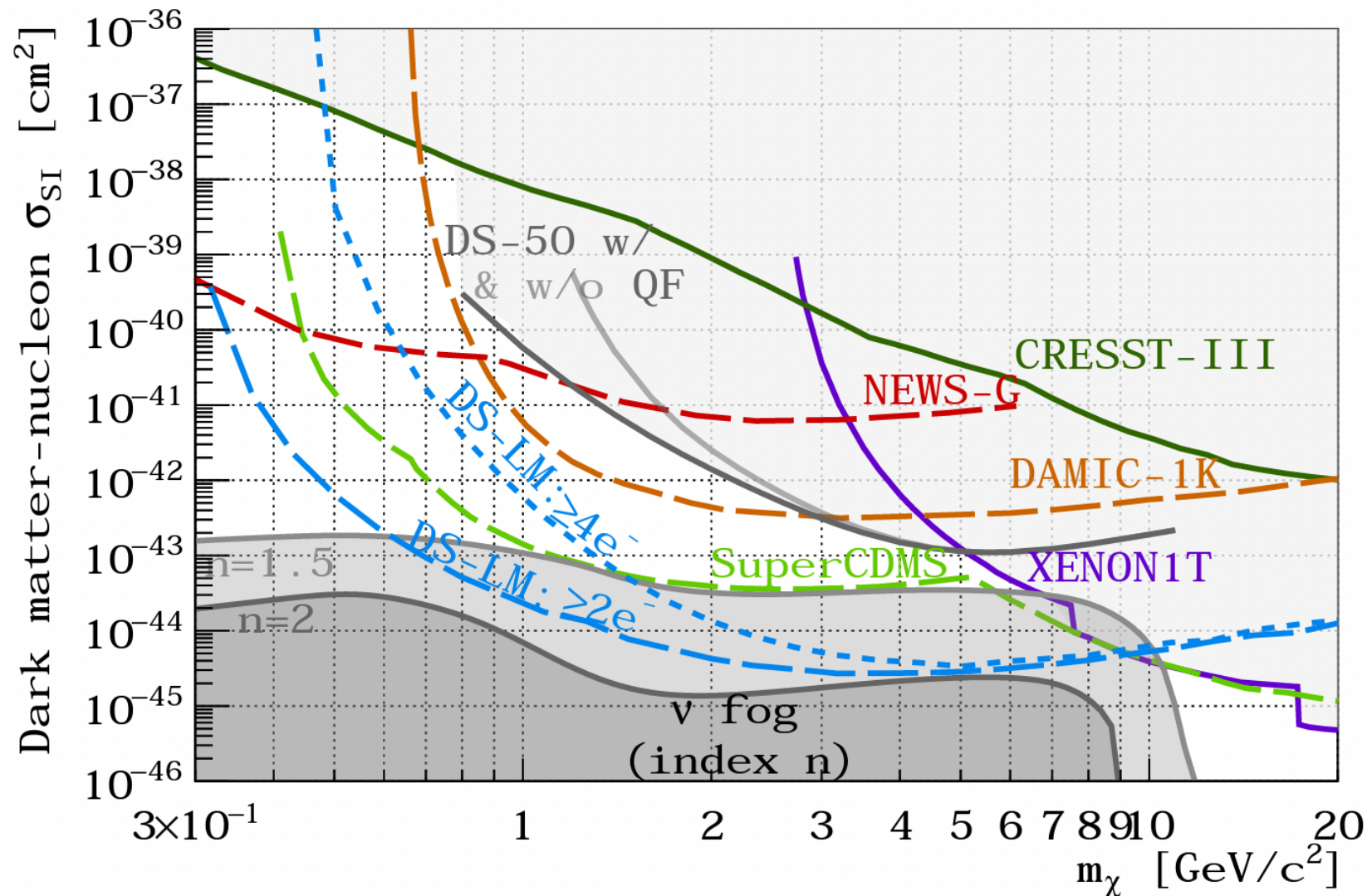


HIGH MASS WIMP SI INTERACTION EXCLUSION LIMITS PROSPECTS

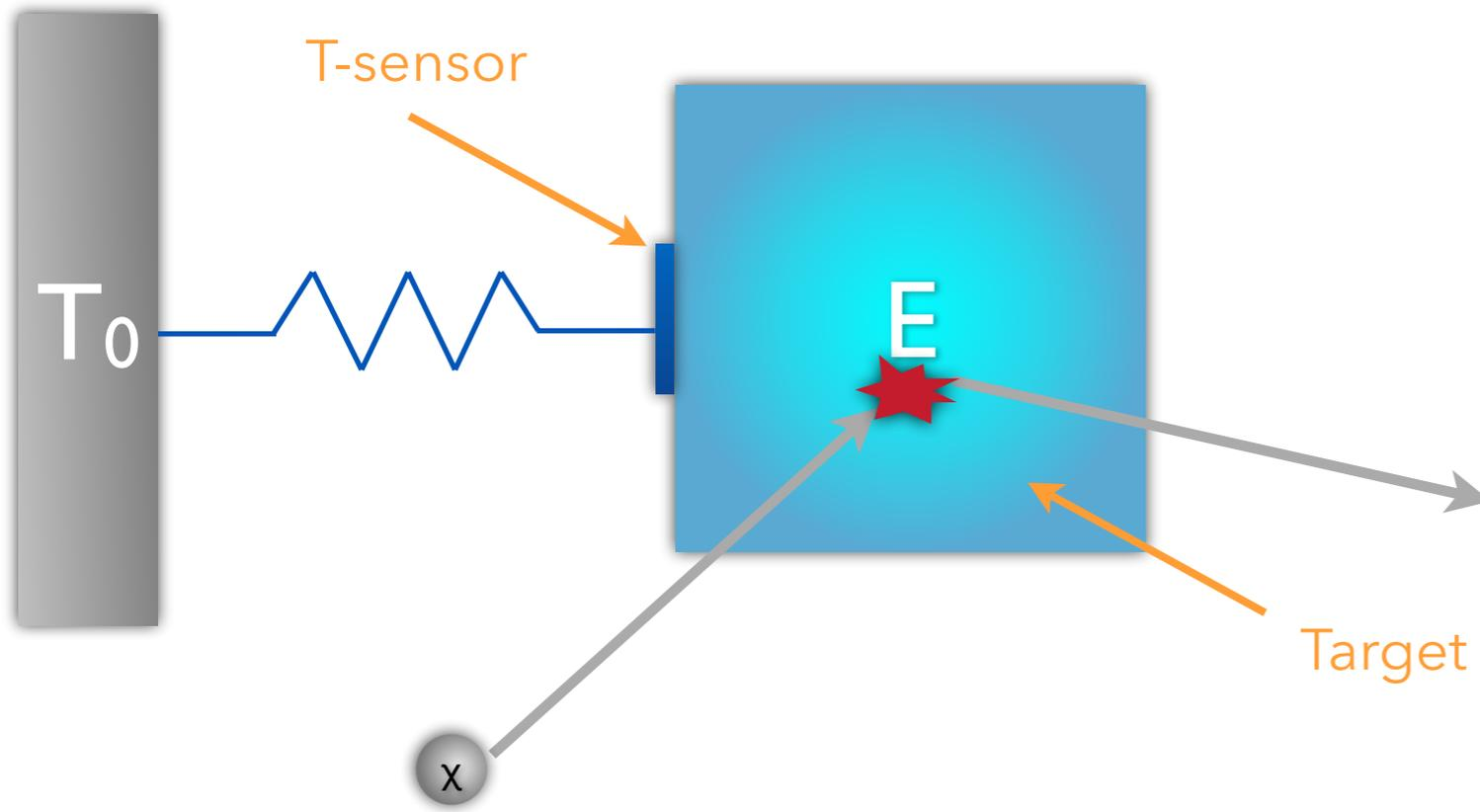


LOW MASS WIMP SI INTERACTION EXCLUSION LIMITS PROSPECTS

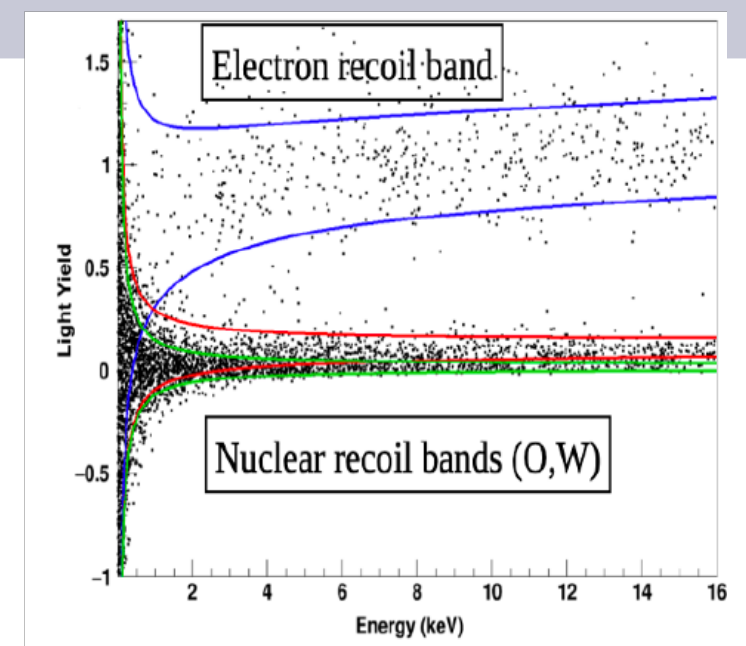
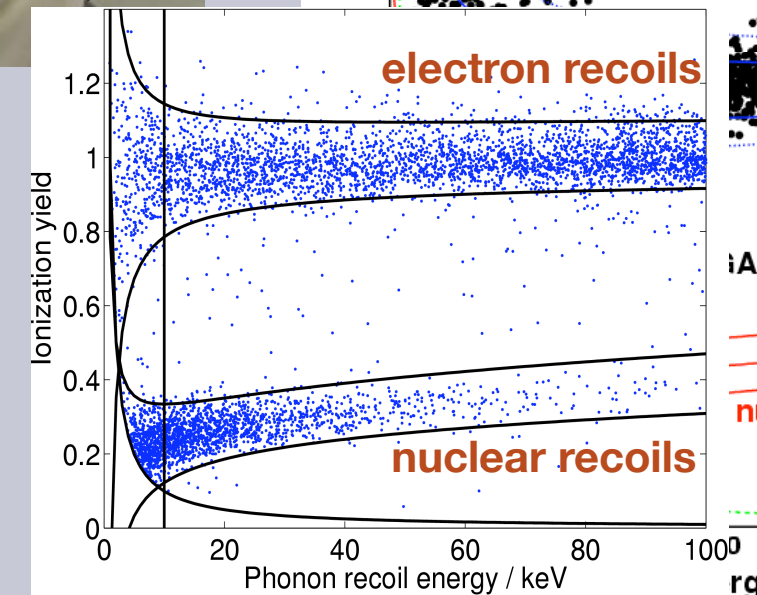
Sensitivity projection for a 1 ton-year exposure dualphase LAr TPC optimized for light dark matter searches through the ionization channel



LOW THRESHOLD: BOLOMETERS



CHARGE & PHONONS:	SUPERCDCMS EDELWEISS
LIGHT & PHONONS:	CRESST COSINUS

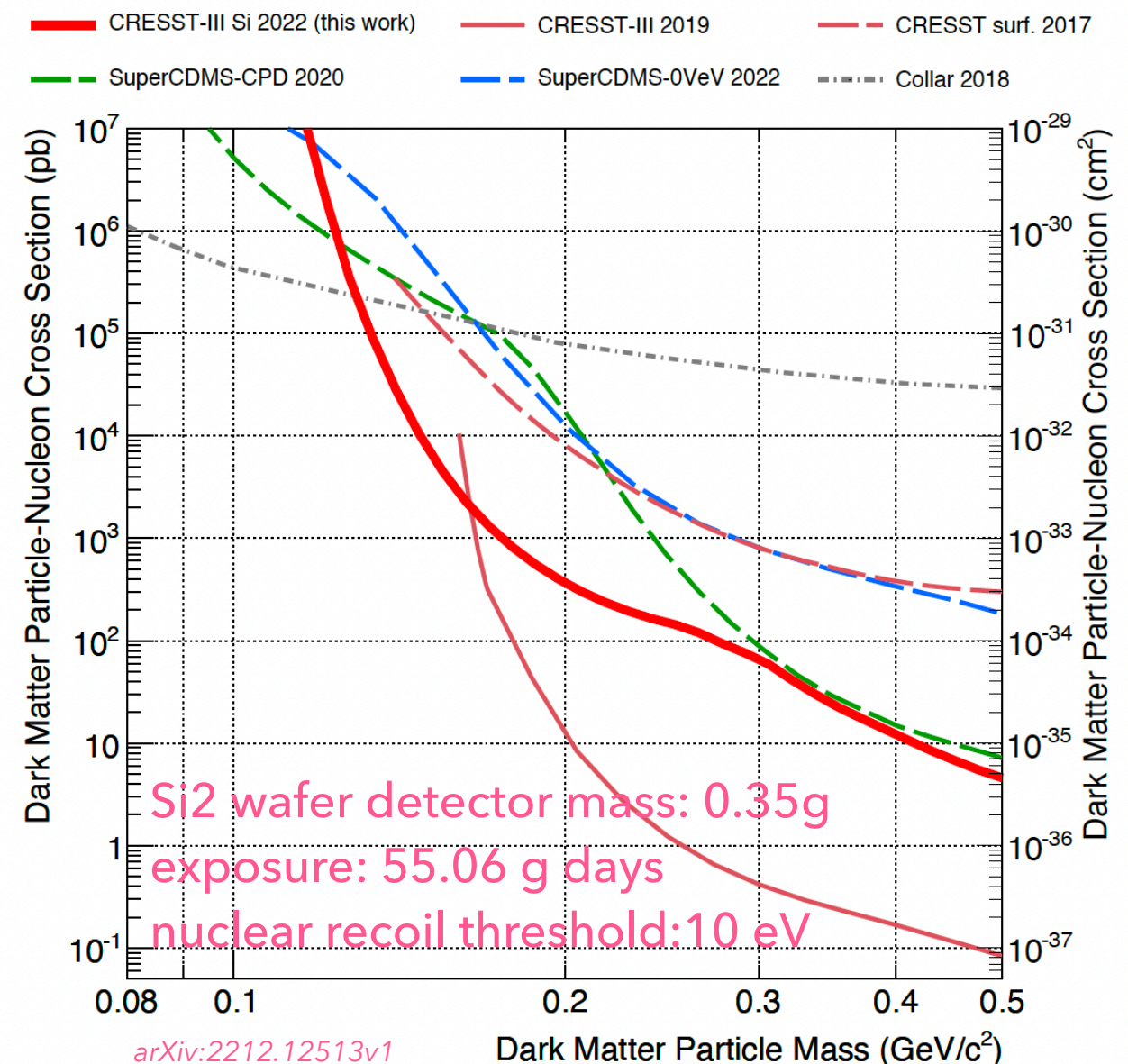
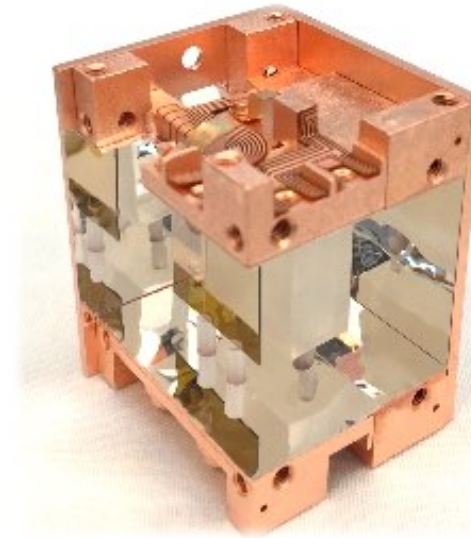


E deposition → temperature rise $\Delta T \sim \mu K$ → requires detectors at mK

- ▶ Sub-keV (< 100 eV) energy thresholds & background discrimination
- ▶ Crystals: Ge, Si, CaWO₄, NaI
- ▶ T-sensors:
 - superconductor thermistors (highly doped superconductor): NTD
Ge → **EDELWEISS**
 - superconducting transition sensors (thin films of SC biased near middle of normal/SC transition): TES → **CDMS, CRESST, COSINUS**

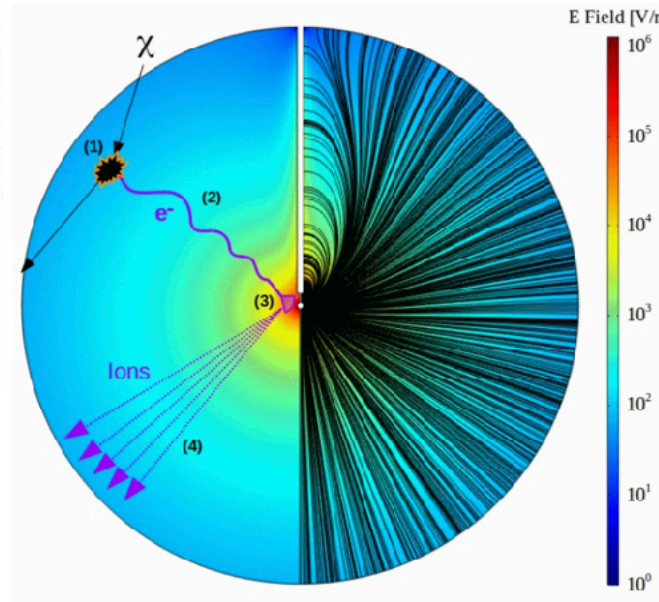
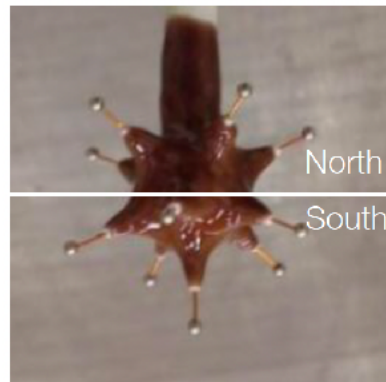
CRESST @LNGS

- ▶ Sub-GeV WIMP mass sensitivity
- ▶ **CRESST-III** run 07/2016 - 02/2018
 - Target crystal mass: 23.6g
 - Gross exposure (before cuts): 5.7 kg days
 - Nuclear recoil threshold: 30 eV
- ▶ Low Energy Excess, still being investigated
 - LEE observed "everywhere", in particular in cryogenic experiments → one single common origin considered unlikely, stress from crystal, sensor or holding.
- ▶ Recent results in the ~100 MeV range for the DM mass and for both SI (Si, CaWO₄) and SD (LiAlO₂) interactions
- ▶ Moving ahead to increase the exposure to consolidate the capability of light DM detection



LOW THRESHOLD: SPC & CCD

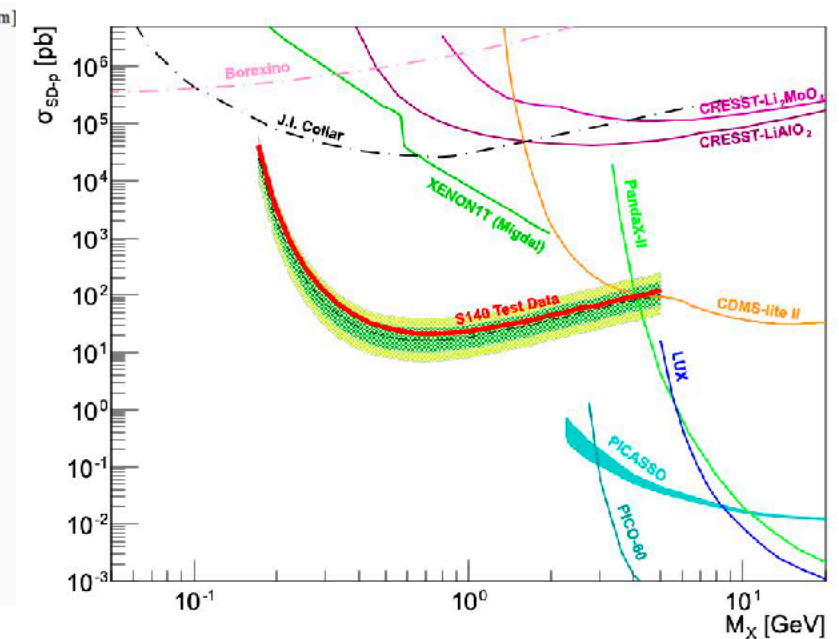
- ▶ **SPC:** spherical proportional counter, light targets (H, He, Ne), pulse shape discrimination against surface events, low energy threshold (very low capacitance)
- ▶ **Skipper CCDs:** low ionization energy, low noise, and particle tracks for background reduction, particle ID (DAMIC-M, SENSEI)



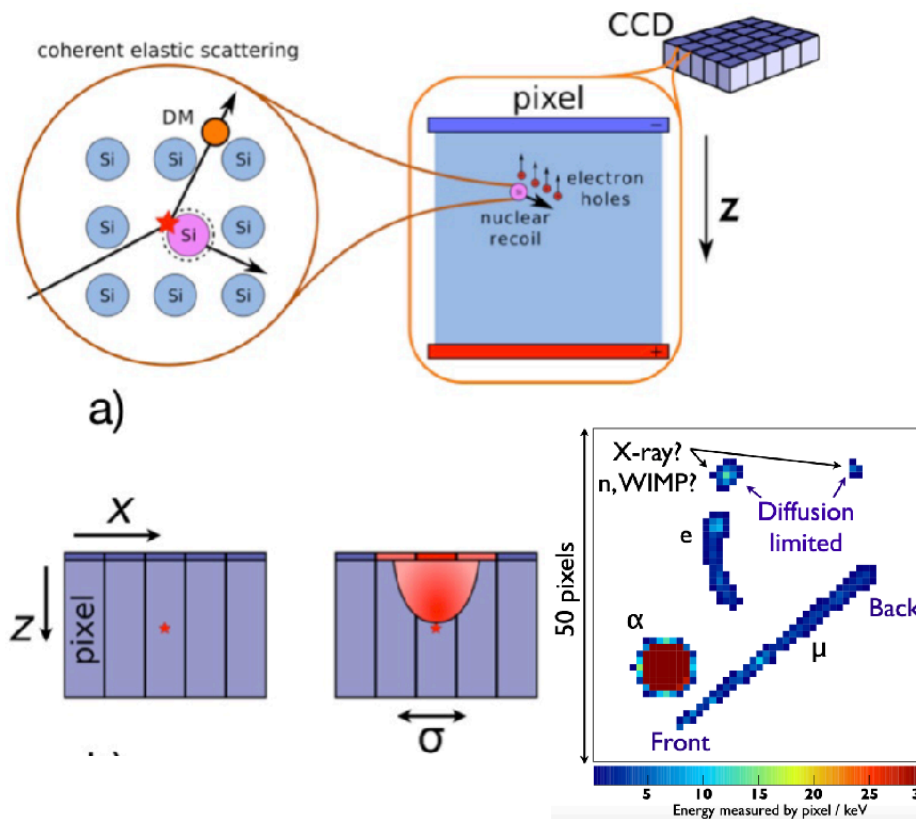
NEWSG @LSM

140 cm diameter copper sphere
135 mbar of pure CH₄ (110 g)

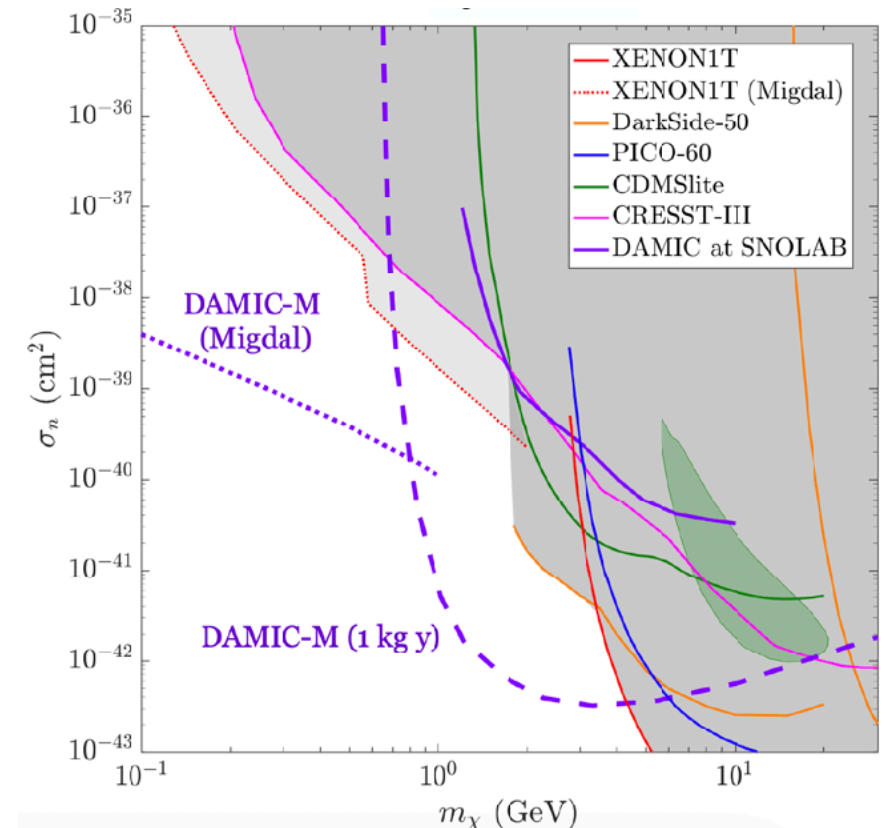
WIMP exclusion limit (S140@LSM, 135mbar CH₄)



D. Durnford UCLA DM 2023



DAMIC-M @LSM



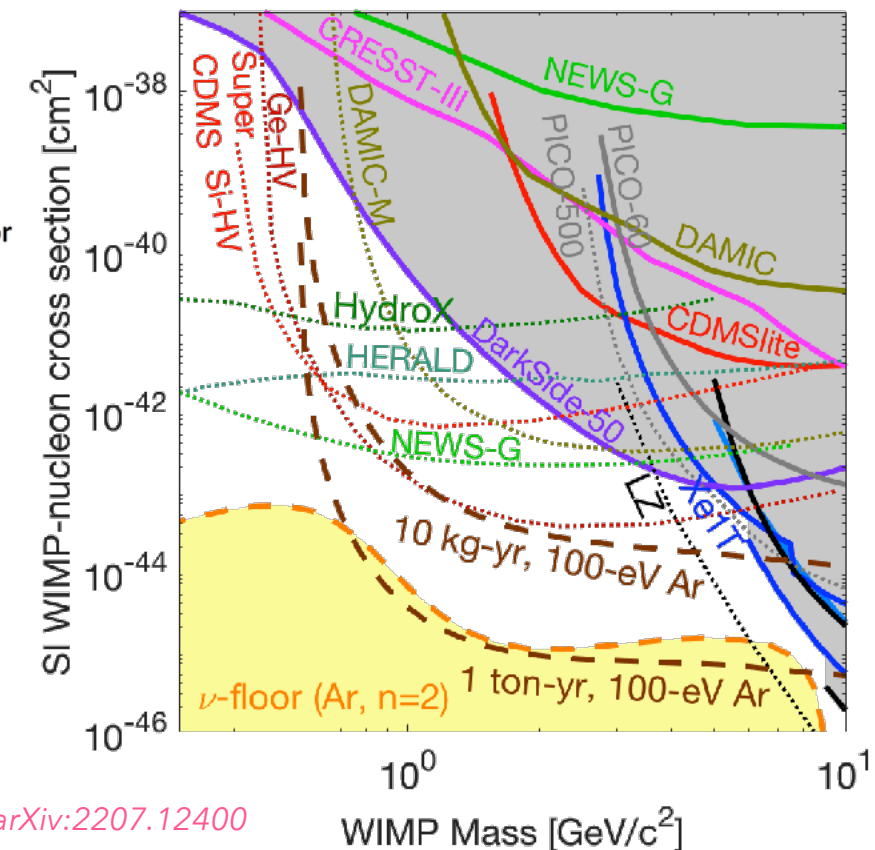
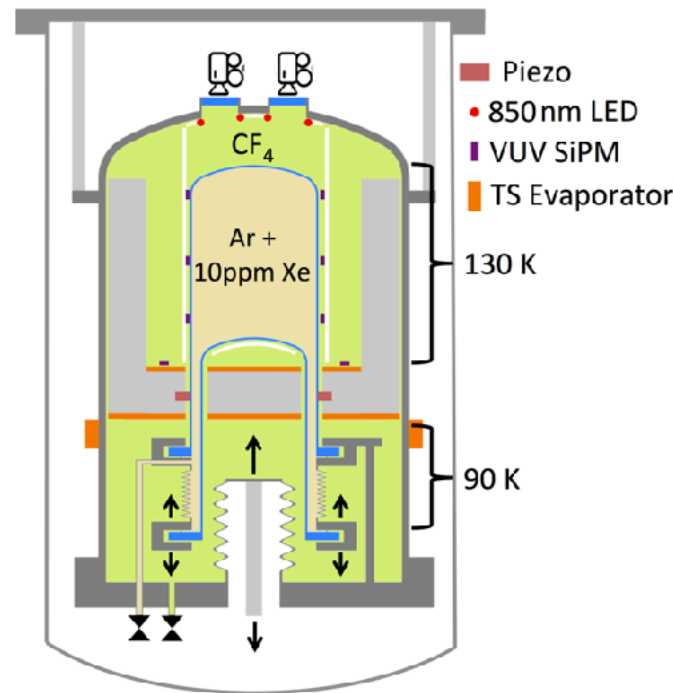
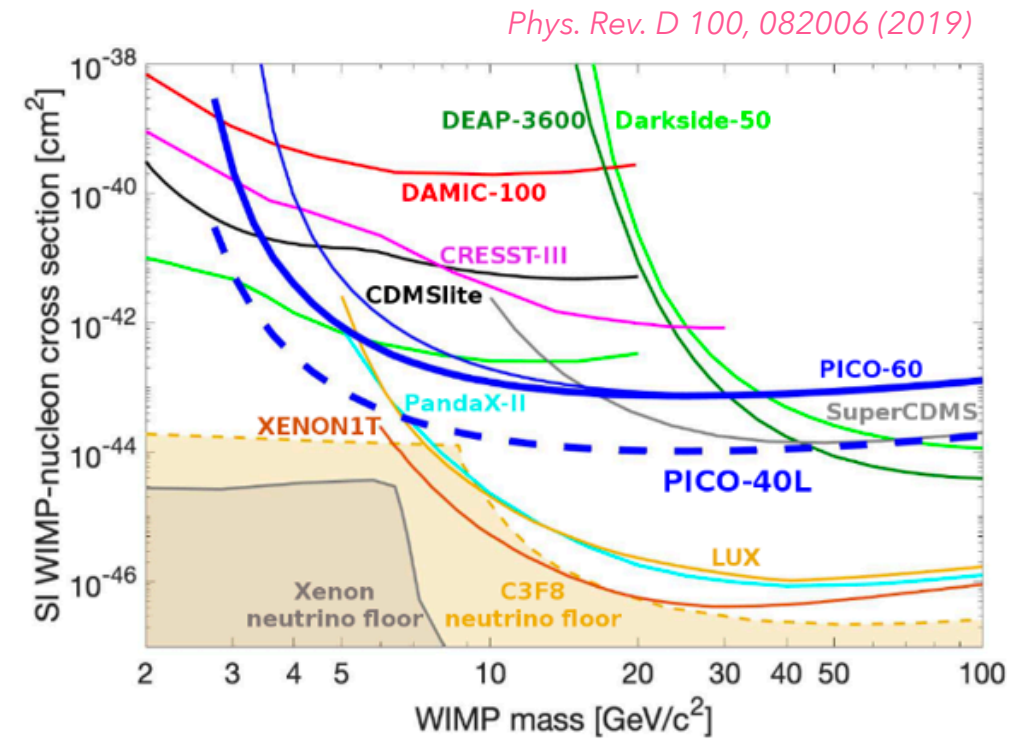
J.-P.Zopounidis UCLA DM 2023

THRESHOLD DETECTORS

Quasi background-free detection of sub-keV nuclear recoils:

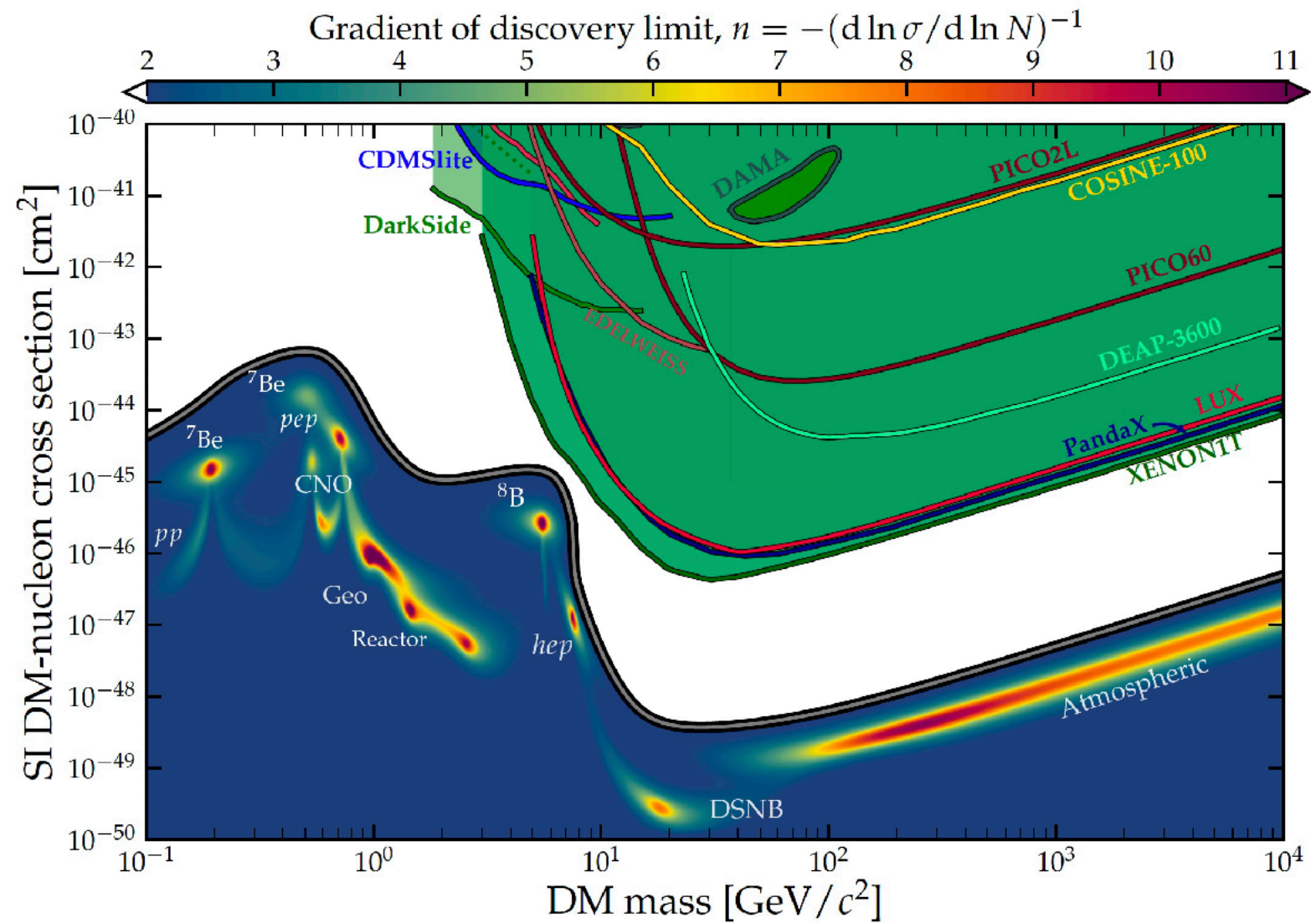
- ▶ Nucleation depends on NR threshold and target fluid:
 - ▶ Freon-based chambers ER-blind @ ~3 keV
 - ▶ Liquid-noble chambers ER-blind @ < 500 eV, (target 100 eV)

- ▶ **PICO** (SNOLAB): superheated freon target, camera + acoustic readout, background rejection based on topology $O(10^{-2})$
 - **PICO-60** SD WIMP-p best limit with 60 kg C_3F_8 target
 - **PICO-40L** new design running
 - **PICO-500** planned
- ▶ **SBC** (SNOLAB): Scintillating Bubble Chamber, superheated 10 kg Xe-doped LAr, cooled to 130 K, piezoelectric sensors + cameras readout + SiPMs for scintillation signal
 - **SBC-LAr10** demonstrator @Fermilab running in 2024, radio pure detector gearing up for first DM search @SNOLAB

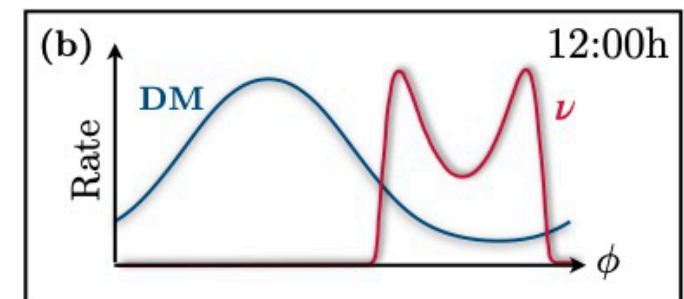
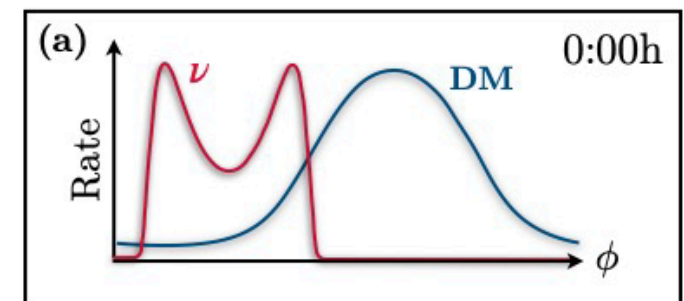
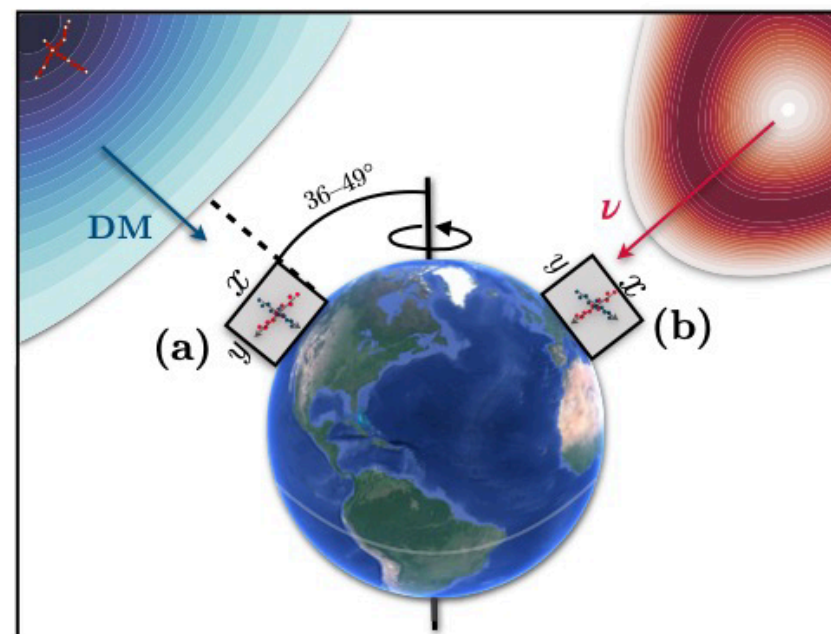


DIRECTIONALITY: THROUGH THE NEUTRINO FOG

- ▶ Directional detectors can separate neutrino and DM signals
- ▶ n remains < 2 even in the neutrino fog
- ▶ fog becomes a positive: a source of guaranteed signal in DM experiment!



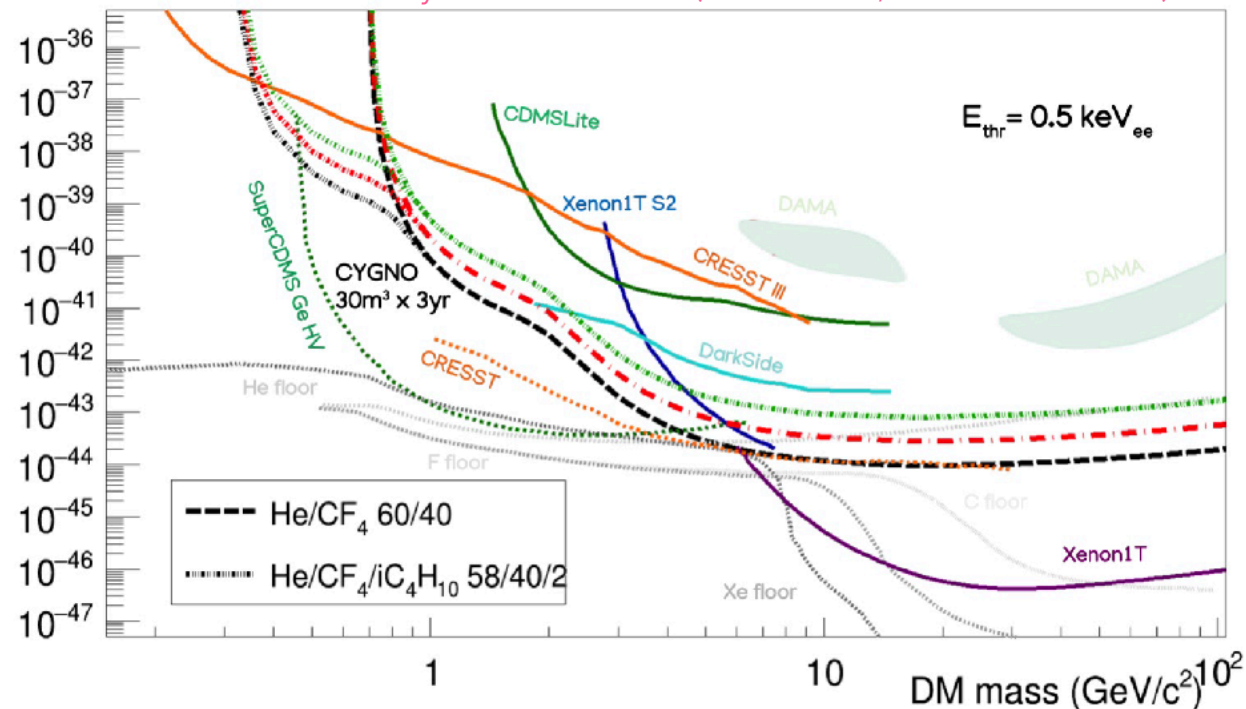
arXiv:2109.03116



DIRECTIONALITY: THROUGH THE NEUTRINO FOG

- ▶ Mature technology: gaseous TPC with different readouts → **CYGNUS (10-1000 m³)**

CYGNUS sensitivity to SI interactions (S. Piacentini, CERN March 2023)



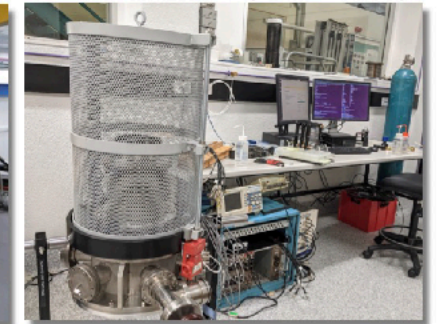
CYGNUS (Italy)



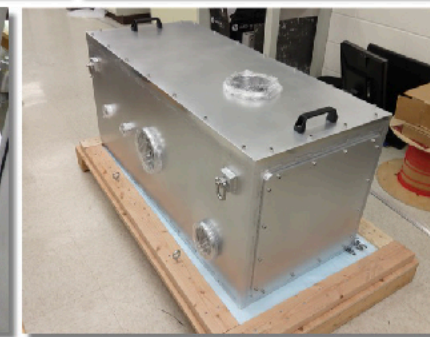
CYGNUS/DRIFT (UK)



CYGNUS-Oz (Australia)



CYGNUS/UNM (USA)



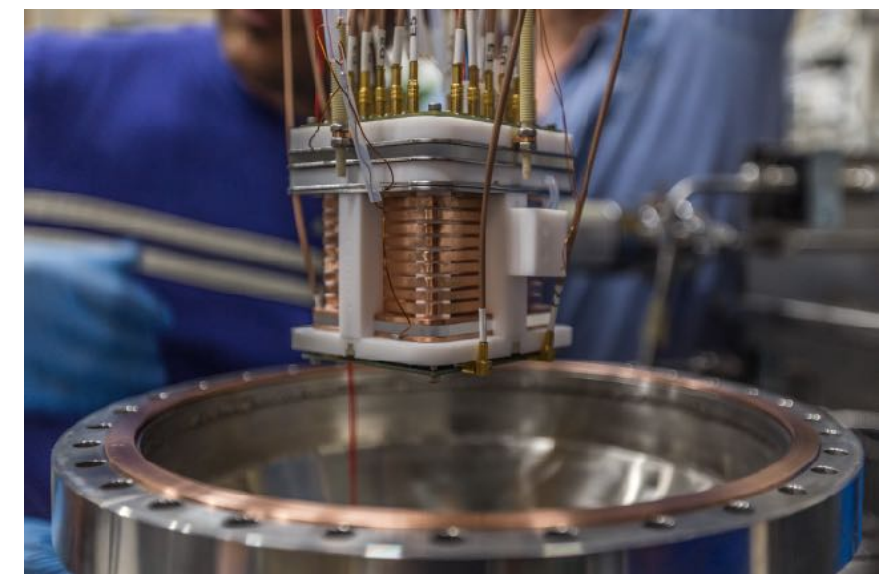
CYGNUS-HD 40 L (USA)



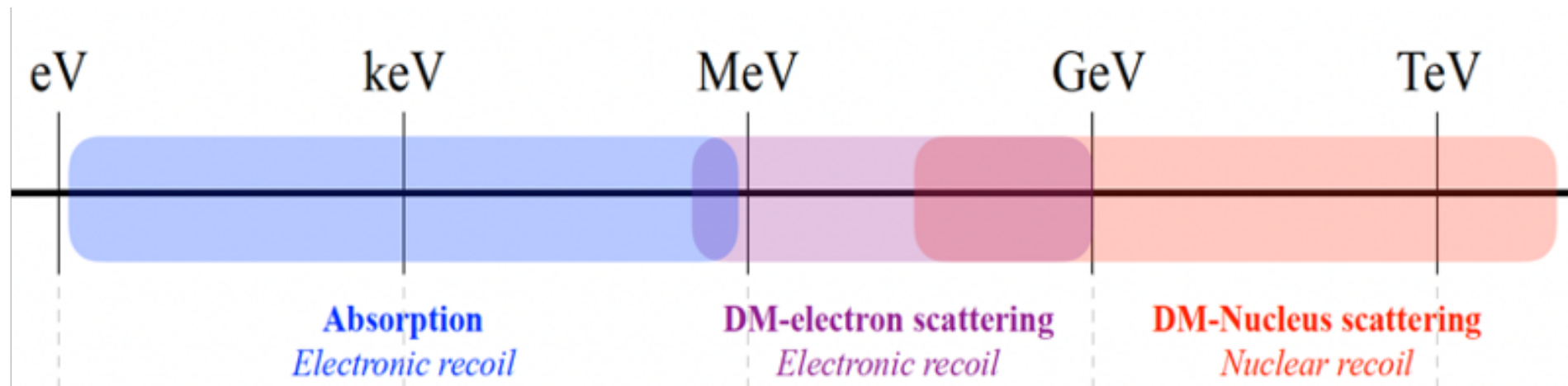
CYGNUS/NEWAGE (Japan)

- ▶ R&D on several other techniques:

- **NEWSdm** Nanometric track direction measurement in nuclear emulsions (exploit resonant light scattering using polarised light)
- **RED** Columnar Recombination in liquid argon TPC
- **PTOLEMY** Graphene target (nanoribbon or nanotubes)



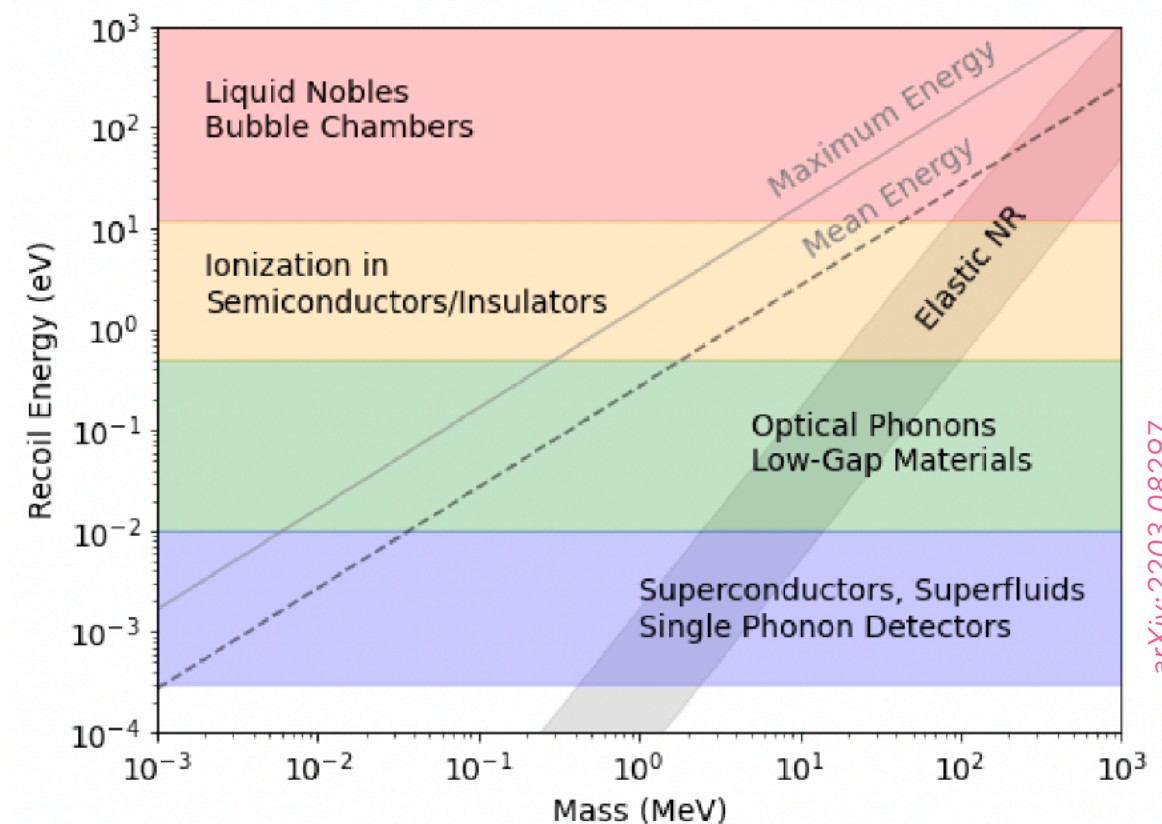
LIGHT DARK MATTER (SUB-GEV)



- ▶ DM mass kinematically accessible through inelastic interactions extracting substantial fraction of the DM kinetic energy:

$$E_{\text{kin}} = \frac{1}{2} m_{\text{DM}} v_{\text{DM}}^2 \sim 1 \text{ eV} \left(\frac{m_{\text{DM}}}{1 \text{ MeV}} \right)$$

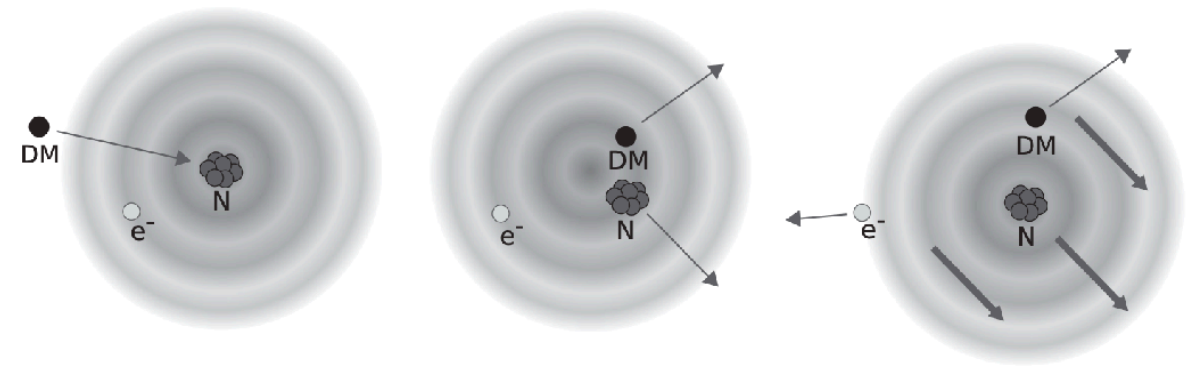
- ◉ DM-N scattering w/ Migdal
- ◉ DM-e scattering
- ◉ DM scattering w/ collective modes (e.g. phonons, magnons)



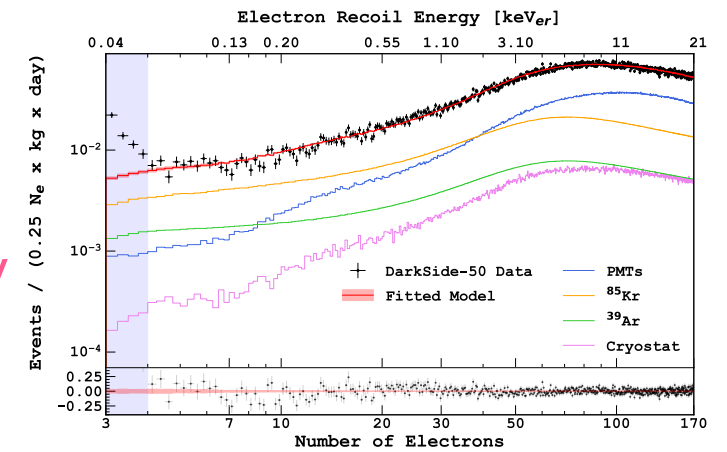
Ibe, et al, JHEP 03 (2018) 194

DM-N SCATTERING w/ MIGDAL

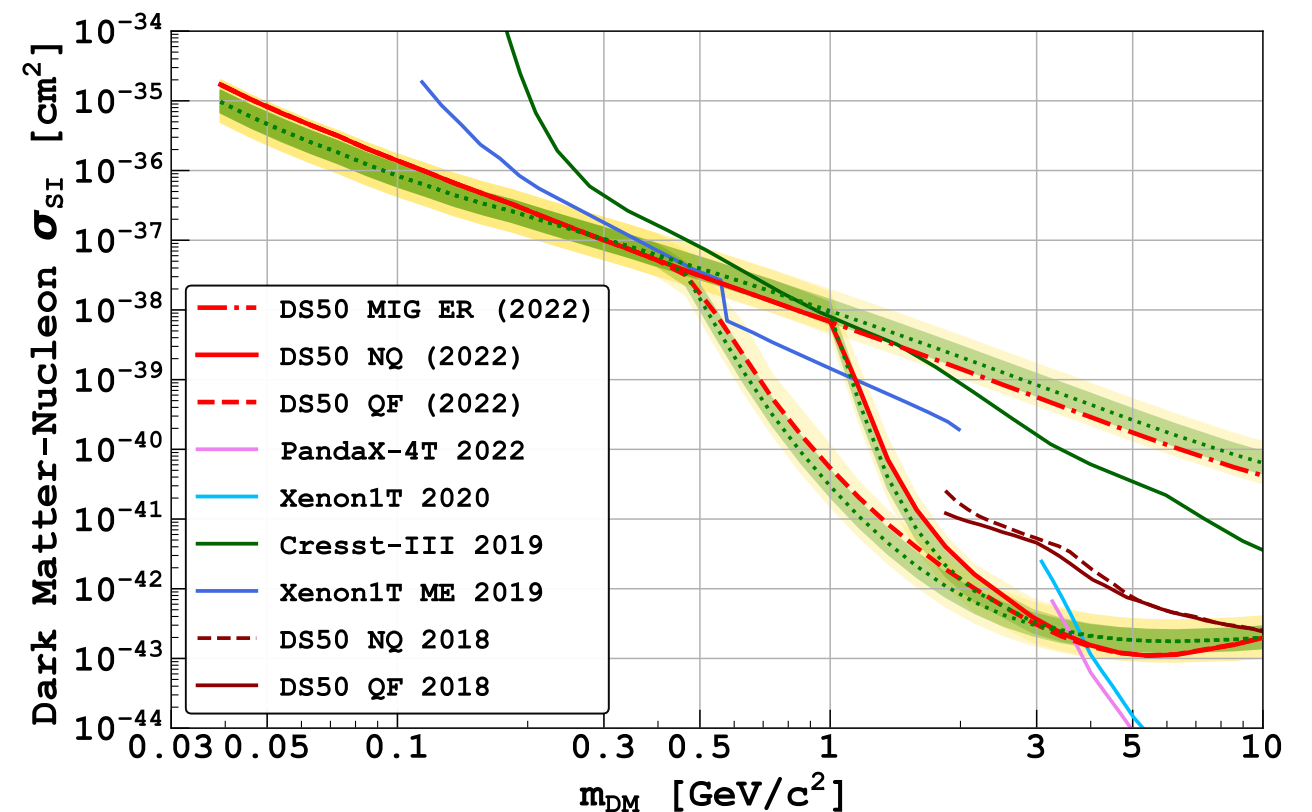
- ▶ Interactions between a neutral particle and a nucleus may result in atomic excitation or ionization
- ▶ Migdal atomic relaxation can lead to keV electron recoil (ER) energy for sub-keV nuclear recoils (NRs)
- ▶ Potential enhancement of low-mass dark matter sensitivity has been explored
 - LUX, PRL 122 131301 (2019)
 - XENON1T, PRL 123 241803 (2019), PRD 106 022001 (2022)
 - DarkSide50, PRL 130 101001 (2023)
 - EDELWEISS, PRD 106 062004 (2022)
 - CDEX-1B, PRL 123 161301 (2019)
 - SuperCDMS, arXiv: 2203.02594
 - and more ...
- ▶ This effect has not been definitively verified
 - ◉ MIGDAL @LLNL: 14.1MeV neutrons on LXe



Analysis based on ionization significantly enhances the sensitivity in sub-GeV region



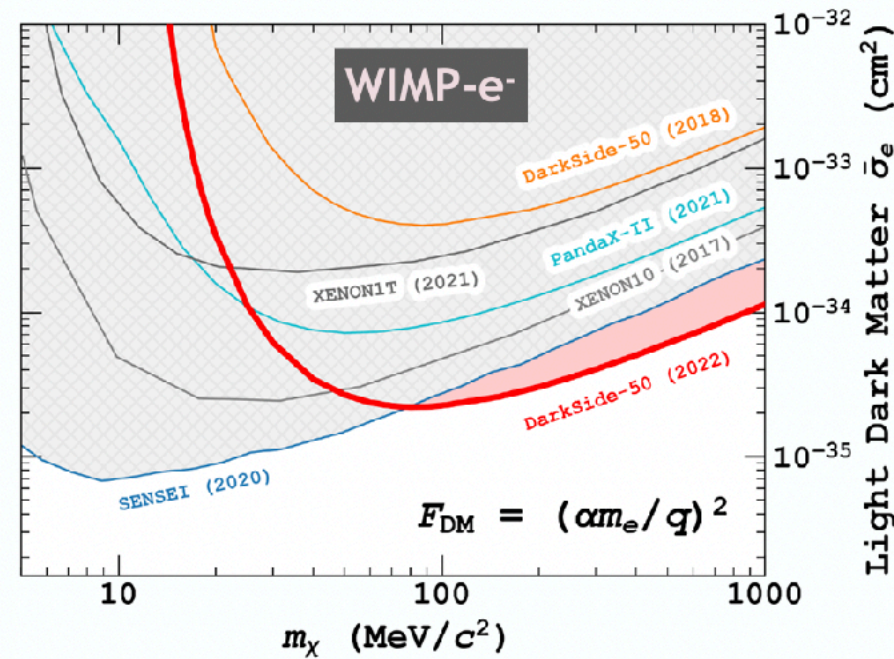
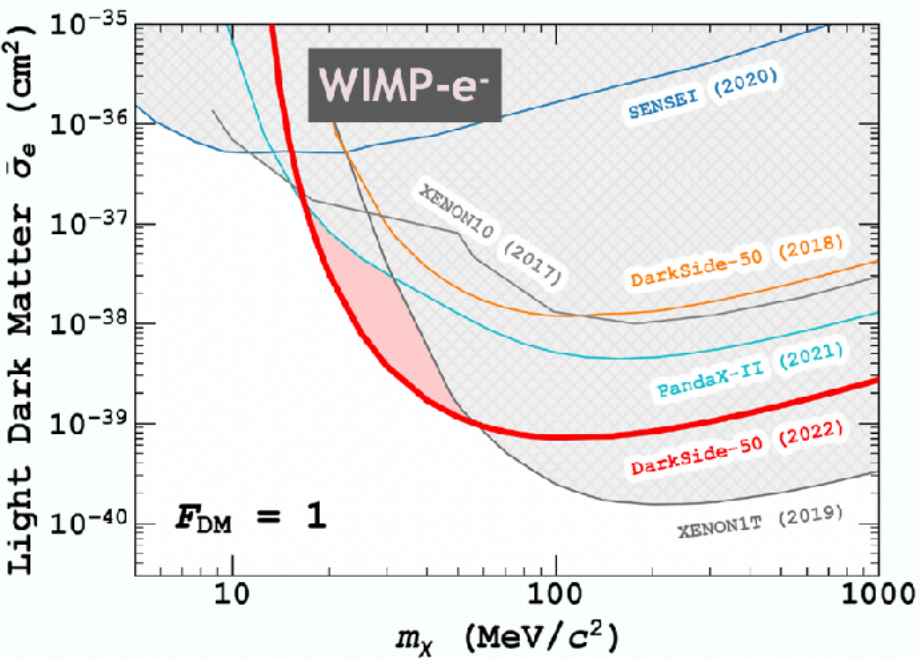
Phys. Rev. D 107, 063001 (2023)



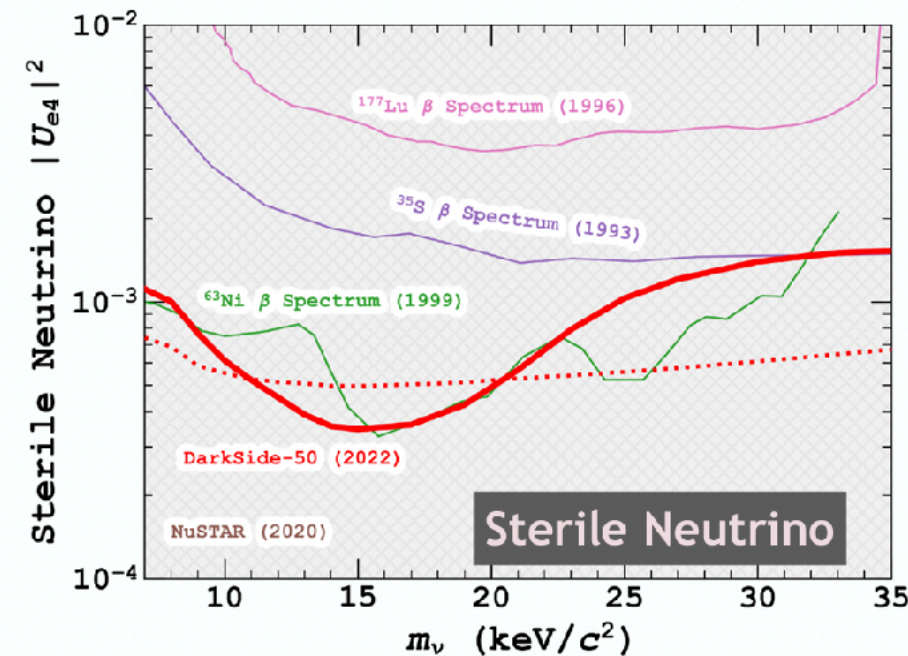
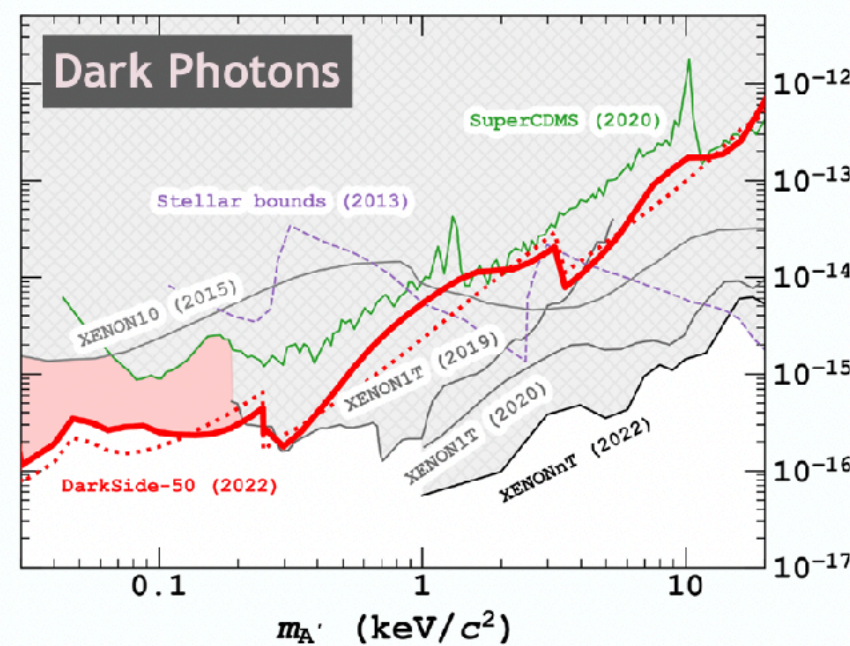
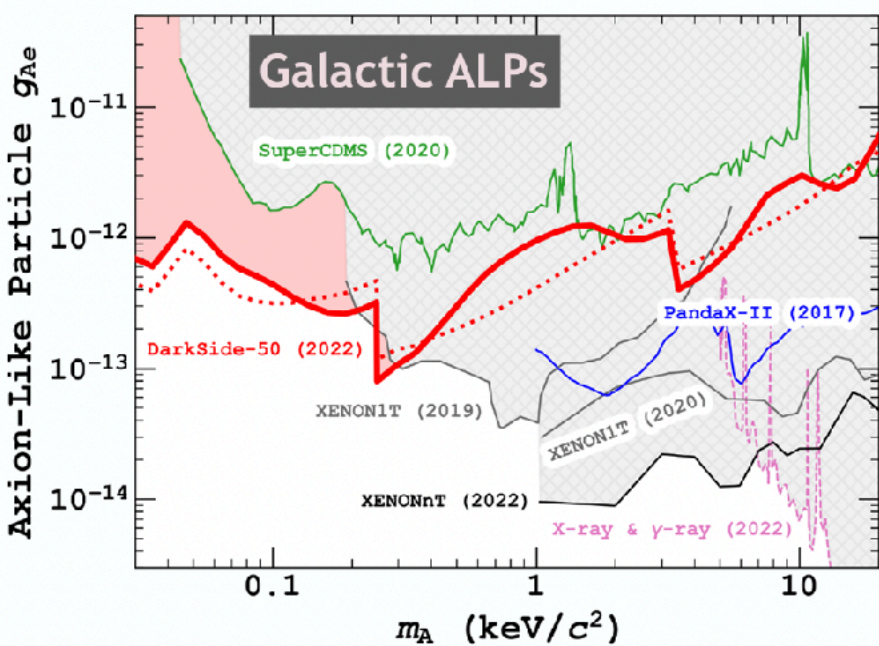
PRL 130, 101001 (2023)

DM-e SCATTERING

Light DM interactions with final state electrons

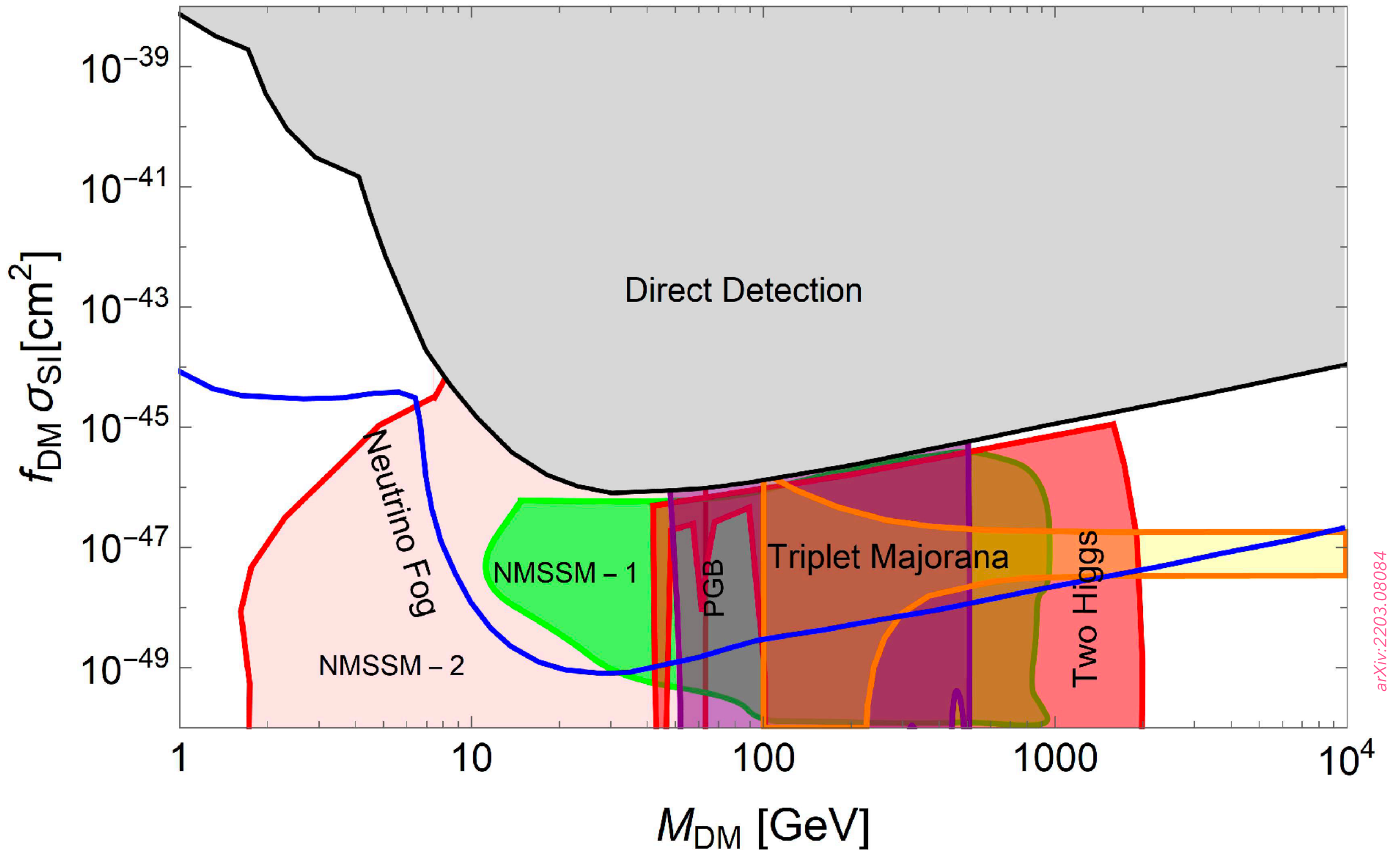


- ▶ light DM-electron scattering
- ▶ absorption of bosonic DM (axion-like particles and dark photons)
- ▶ sterile neutrino-electron scattering



WHAT NEXT?

predictions for SI scattering cross sections (in plots of DM-proton cross section versus DM mass) for visible sector models

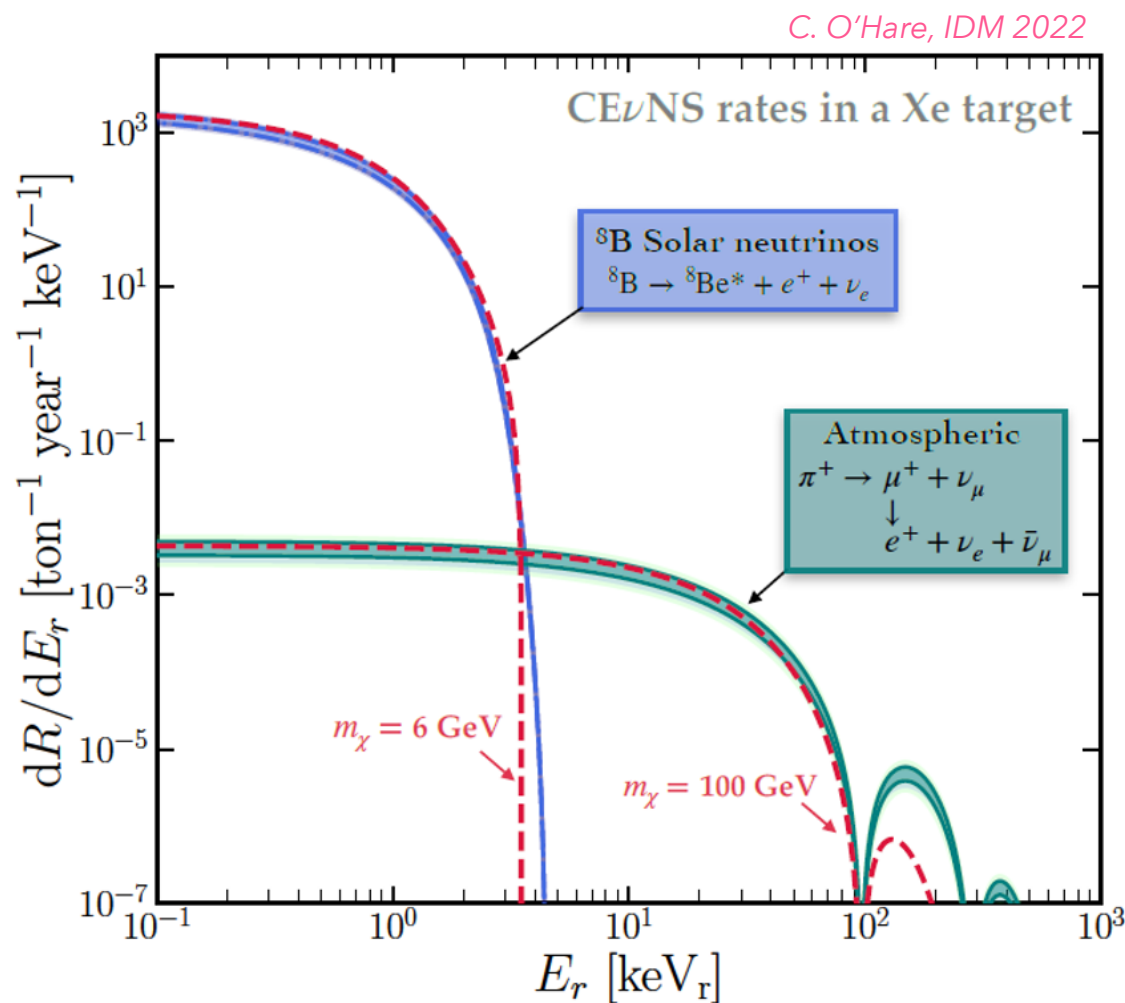


SUMMARY & OUTLOOK

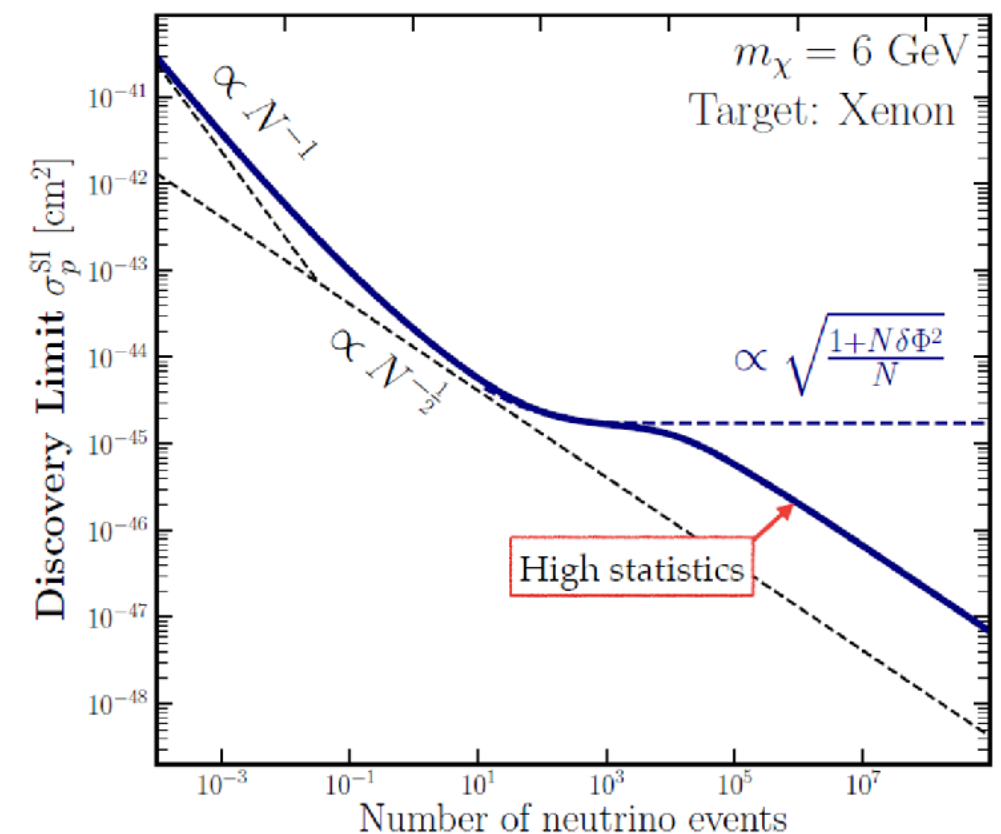
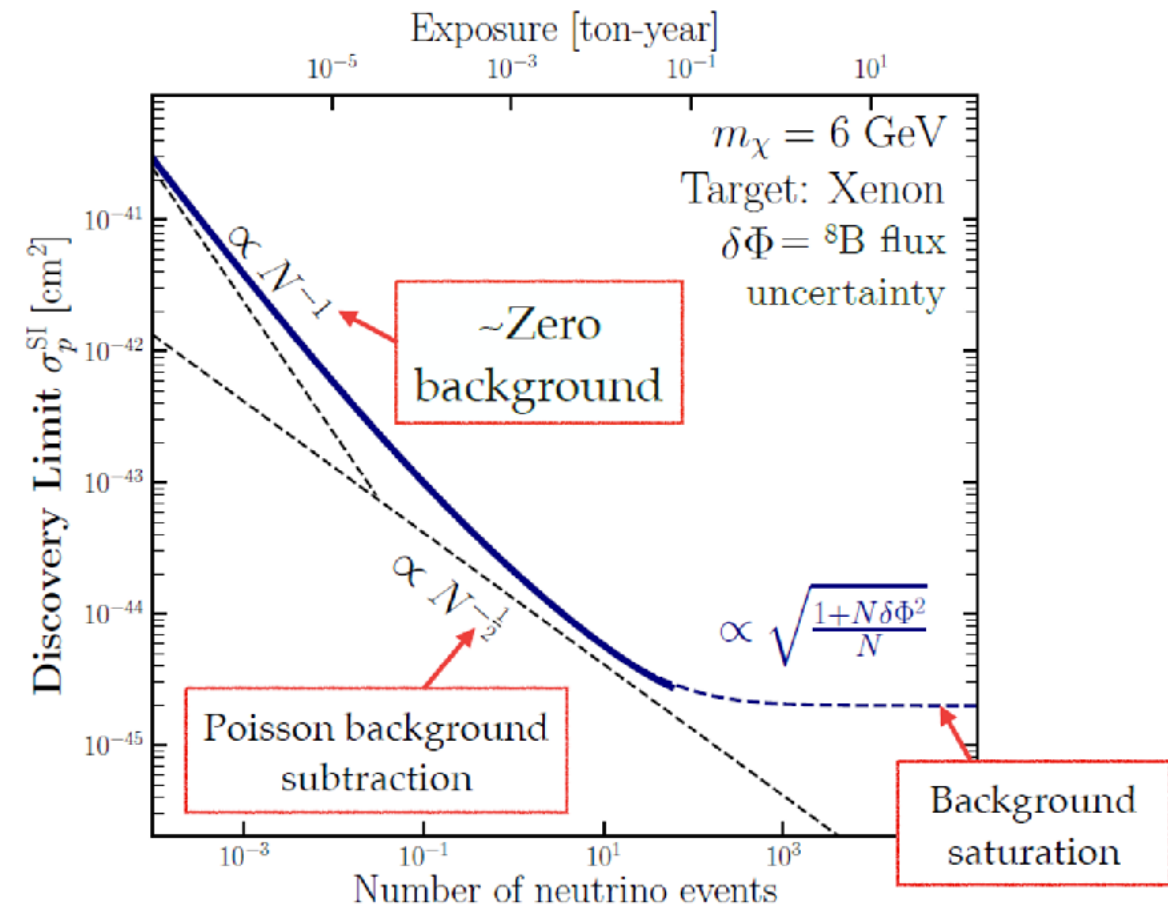
- ❖ Direct dark matter detection experiments need to explore everywhere
- ❖ WIMP still main paradigm: a variety of detector technologies in place to reach ν fog, add directional sensitivity to clear it
- ❖ Light DM probed via scattering to 1 MeV (and via absorption to \sim eV), and possibly much lower
- ❖ *Ultra Light DM: a wealth of dedicated initiatives probing sub-eV masses (not covered here...)*

ADDITIONAL SLIDES

IRREDUCIBLE BACKGROUND: NEUTRINOS



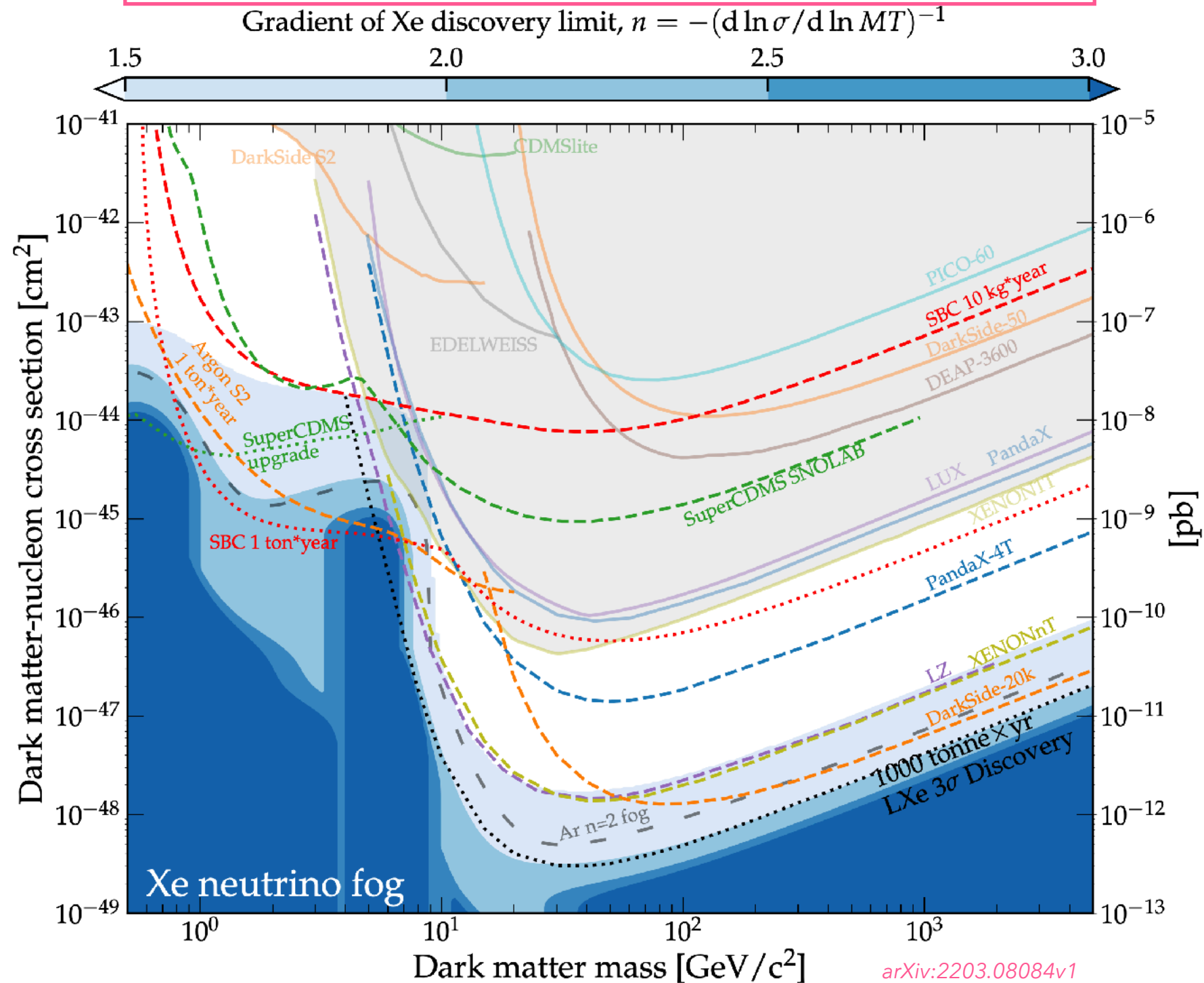
- ▶ Coherent nuclear recoils from several astrophysical sources (Sun, atmosphere, and diffuse Supernovae)
- ▶ DM/CEvNS signals not identical \rightarrow with high statistics, an experiment can overcome background uncertainty using spectral information



NEUTRINO FOG

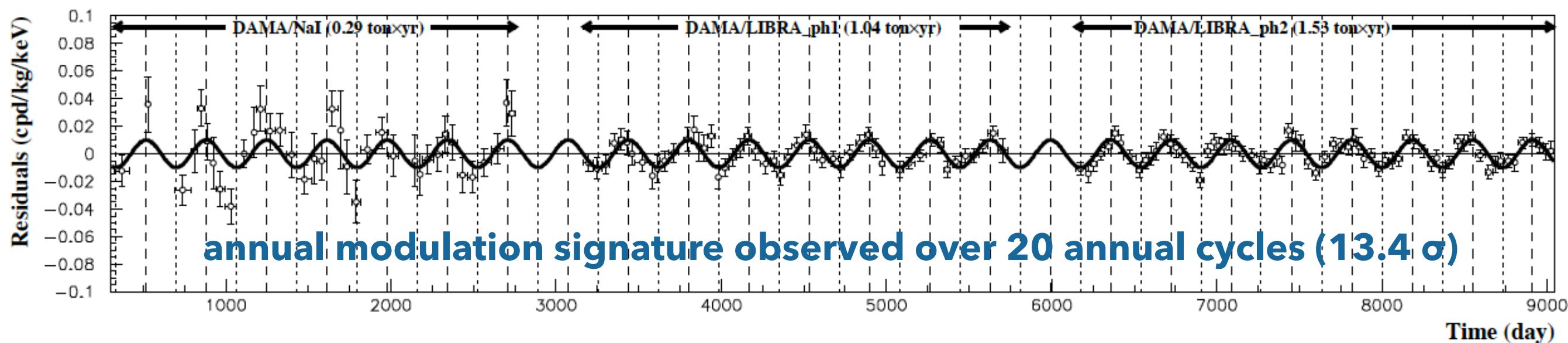
- ▶ Neutrino floor from CEvNS not a hard limit on direct detection sensitivity, rather a gradual penalty that can be overcome to some extent.
- ▶ To clear the fog:
 - increase exposures
 - have multiple target nuclei
 - improve neutrino flux measurements
 - use signatures

The n index quantifies the diminishing gain in increasing exposure when limited by neutrinos: reducing the sensitivity by a factor of 10 requires increasing the exposure by at least 10^n



DAMA MODULATION SIGNAL

- ▶ Standard Halo Model predicted modulation $A \sim 0.02-0.1$, $t_0 = 152.5$ days
- ▶ **DAMA/NaI + DAMA/LIBRA-phase1 + phase2:**
 - 2.86 t × yr (2 – 6 keV)
 - $A = (0.00996 \pm 0.00074)$ cpd/kg/keV $\chi^2/\text{dof} = 130/155$



No signal from other direct detection experiments

ANAIS-112 (LSC) & COSINE-100 (Y2L) offer direct test, no clear observation of modulation

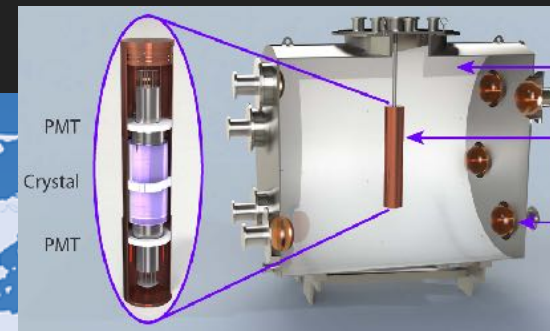
DAMA/LIBRA-phase2-empowered running with lower software energy threshold of 0.5 keV

MODEL INDEPENDENT CHECK

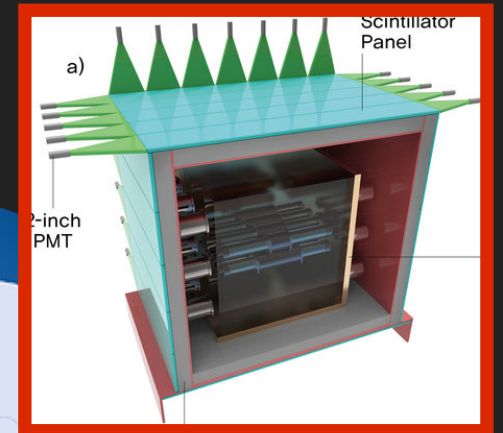
ANAIS-112



SABRE NORTH

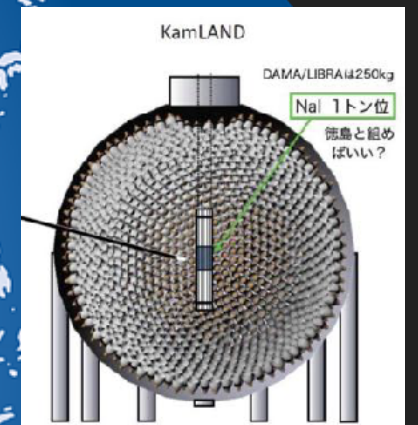


COSINE-100



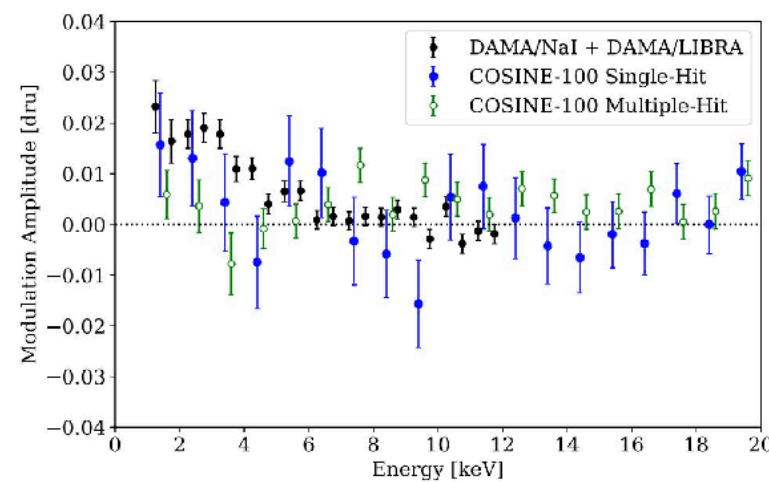
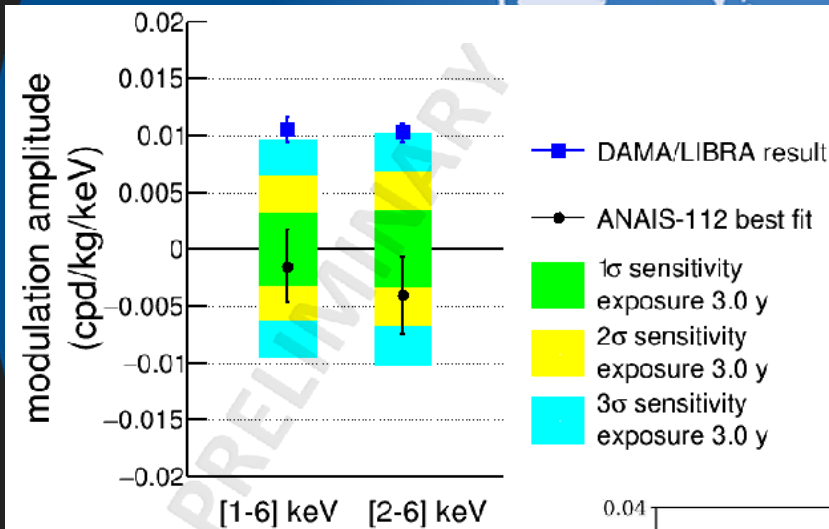
COSINUS

PICOLON



SABRE SOUTH

TAKING DATA



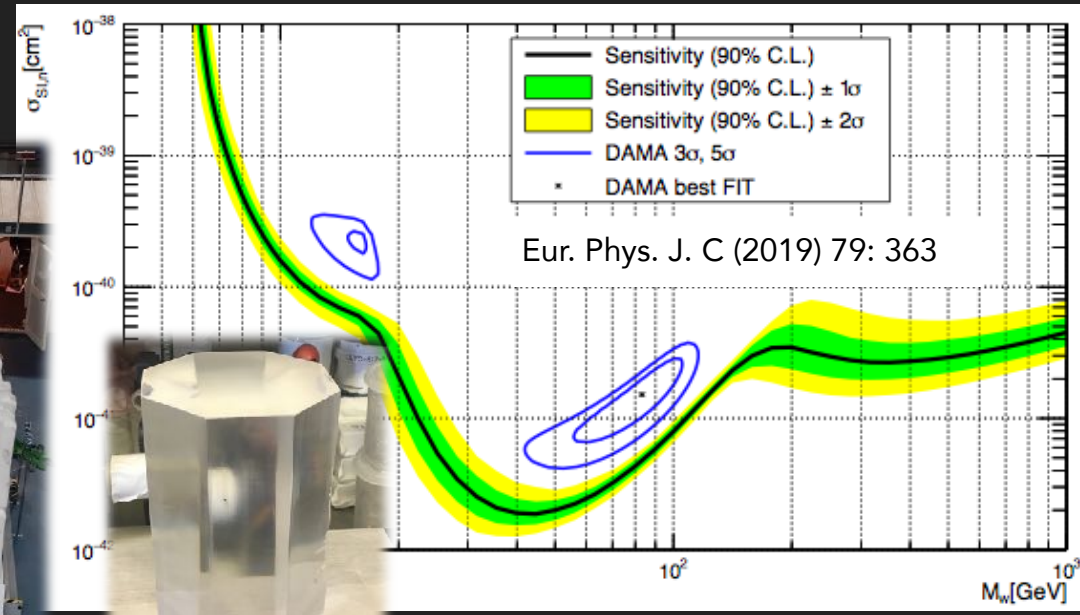
ANAIS-112,
UCLA DM 2023

COSINE-100,
Phys. Rev. D. 106, 052005

MODULATION PERSPECTIVE (@LNGS)

SABRE

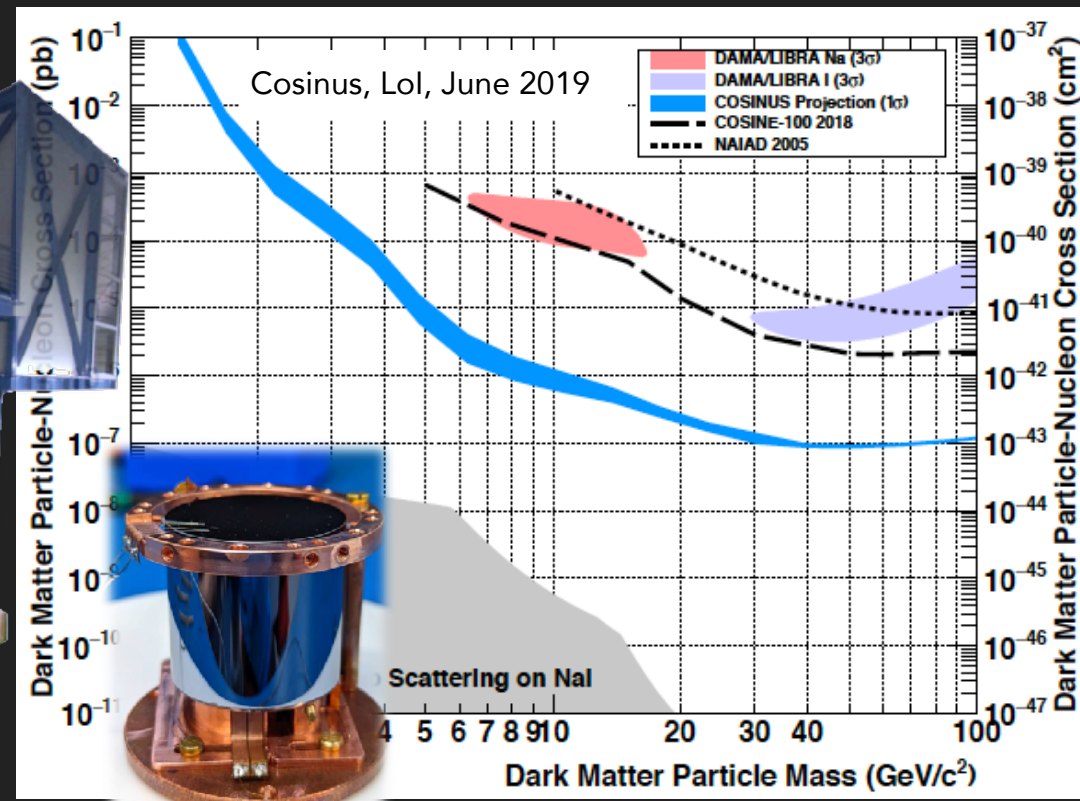
- ▶ Development of ultra-high purity NaI(Tl) crystals (3-5 kg, 0.1-0.3 dru in the ROI)
 - ▶ PoP at LNGS exploited successfully ^{40}K tagging with sensitivity at the level of 1ppb
- ▶ Two sites: LNGS in Northern and SUPL in Southern hemisphere
 - ▶ Passive shielding (North) + active veto (South)



exposure of 150 kg yrs

COSINUS

- ▶ NaI detectors operated as cryogenic calorimeters
- ▶ dual readout of heat and scintillation light
- ▶ construction phase, several prototypes, mass 60g \rightarrow 110g
- ▶ COSINUS-1p: $\mathcal{O}(100 \text{ kg days})$ to know whether DAMA sees a nuclear recoil signal or not (low threshold essential)

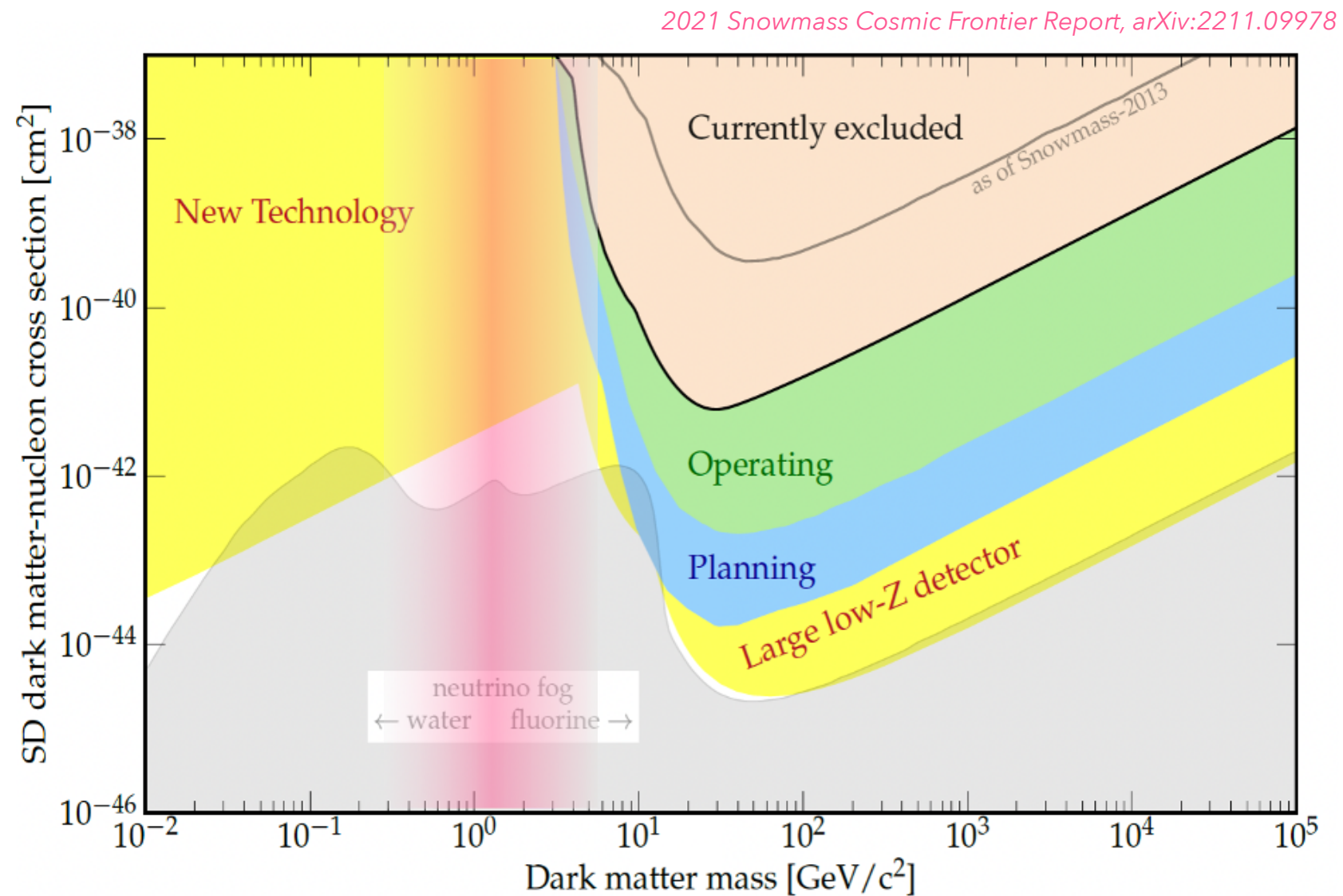


exposure of 100 kg days

WIMP NUCLEON SD INTERACTION EXCLUSION LIMITS LANDSCAPE

► Spin-dependent phase space is wide-open at lower masses but technology to probe deep at 10 - 100 GeV/c² is well-developed

- **PICO** superheated bubble chambers Freon (C₃F₈) probe proton coupling
- **LXe TPC** detectors cover n-coupling, but the xenon neutrino fog is decades higher than the fluorine neutrino fog
- **EDELWEISS, SuperCDMS** n-coupling at lower masses **CRESST** is exploring new SD crystals with Lithium
- New technology could be a liquid/solid phase change detector like supercooled H₂O



WIMP-NUCLEON SCATTERING IN NREFT

- ▶ More general description by non-relativistic effective field theory
- ▶ expansion parameters: $v/c \simeq 10^{-3}$ and $|\vec{q}|/m_M$
- ▶ $|\vec{q}| \simeq \mathcal{O}(10 - 100 \text{ MeV})$ is the momentum exchange
- ▶ m_M is some large scale involved (DM mass, nucleus mass, or a heavy mediator mass)

relativistic interactions constructed as bilinear products of the available scalar and four-vector amplitudes (20 effective Lagrangians)

j	$\mathcal{L}_{\text{int}}^j$	Nonrelativistic reduction	$\sum_i c_i \mathcal{O}_i$	P/T
1	$\bar{\chi}\chi\bar{N}N$	$1_\chi 1_N$	\mathcal{O}_1	E/E
2	$i\bar{\chi}\chi\bar{N}\gamma^5 N$	$i\frac{\vec{q}}{m_N} \cdot \vec{S}_N$	\mathcal{O}_{10}	O/O
3	$i\bar{\chi}\gamma^5\chi\bar{N}N$	$-i\frac{\vec{q}}{m_\chi} \cdot \vec{S}_\chi$	$-\frac{m_N}{m_\chi}\mathcal{O}_{11}$	O/O
4	$\bar{\chi}\gamma^5\chi\bar{N}\gamma^5 N$	$-\frac{\vec{q}}{m_\chi} \cdot \vec{S}_\chi \frac{\vec{q}}{m_N} \cdot \vec{S}_N$	$-\frac{m_N}{m_\chi}\mathcal{O}_6$	E/E
5	$\bar{\chi}\gamma^\mu\chi\bar{N}\gamma_\mu N$	$1_\chi 1_N$	\mathcal{O}_1	E/E
6	$\bar{\chi}\gamma^\mu\chi\bar{N}i\sigma_{\mu\alpha}\frac{q^\alpha}{m_M}N$	$\frac{\vec{q}^2}{2m_N m_M}1_\chi 1_N + 2(\frac{\vec{q}}{m_\chi} \times \vec{S}_\chi + i\vec{v}^\perp) \cdot (\frac{\vec{q}}{m_M} \times \vec{S}_N)$	$\frac{\vec{q}^2}{2m_N m_M}\mathcal{O}_1 - 2\frac{m_N}{m_M}\mathcal{O}_3 + 2\frac{m_N^2}{m_M m_\chi}(\frac{\vec{q}^2}{m_N^2}\mathcal{O}_4 - \mathcal{O}_6)$	E/E
7	$\bar{\chi}\gamma^\mu\chi\bar{N}\gamma_\mu\gamma^5 N$	$-2\vec{S}_N \cdot \vec{v}^\perp + \frac{2}{m_\chi}i\vec{S}_\chi \cdot (\vec{S}_N \times \vec{q})$	$-2\mathcal{O}_7 + 2\frac{m_N}{m_\chi}\mathcal{O}_9$	O/E
8	$i\bar{\chi}\gamma^\mu\chi\bar{N}i\sigma_{\mu\alpha}\frac{q^\alpha}{m_M}\gamma^5 N$	$2i\frac{\vec{q}}{m_M} \cdot \vec{S}_N$	$2\frac{m_N}{m_M}\mathcal{O}_{10}$	O/O
9	$\bar{\chi}i\sigma^{\mu\nu}\frac{q_\nu}{m_M}\chi\bar{N}\gamma_\mu N$	$-\frac{\vec{q}^2}{2m_\chi m_M}1_\chi 1_N - 2(\frac{\vec{q}}{m_N} \times \vec{S}_N + i\vec{v}^\perp) \cdot (\frac{\vec{q}}{m_M} \times \vec{S}_\chi)$	$-\frac{\vec{q}^2}{2m_\chi m_M}\mathcal{O}_1 + \frac{2m_N}{m_M}\mathcal{O}_5 - 2\frac{m_N^2}{m_M}(\frac{\vec{q}^2}{m_N^2}\mathcal{O}_4 - \mathcal{O}_6)$	E/E
10	$\bar{\chi}i\sigma^{\mu\nu}\frac{q_\nu}{m_M}\chi\bar{N}i\sigma_{\mu\alpha}\frac{q^\alpha}{m_M}N$	$4(\frac{\vec{q}}{m_M} \times \vec{S}_\chi) \cdot (\frac{\vec{q}}{m_M} \times \vec{S}_N)$	$4(\frac{\vec{q}^2}{m_M^2}\mathcal{O}_4 - \frac{m_N^2}{m_M^2}\mathcal{O}_6)$	E/E
11	$\bar{\chi}i\sigma^{\mu\nu}\frac{q_\nu}{m_M}\chi\bar{N}\gamma^\mu\gamma^5 N$	$4i(\frac{\vec{q}}{m_M} \times \vec{S}_\chi) \cdot \vec{S}_N$	$4\frac{m_N}{m_M}\mathcal{O}_9$	O/E
12	$i\bar{\chi}i\sigma^{\mu\nu}\frac{q_\nu}{m_M}\chi\bar{N}i\sigma_{\mu\alpha}\frac{q^\alpha}{m_M}\gamma^5 N$	$-[i\frac{\vec{q}^2}{m_\chi m_M} - 4\vec{v}^\perp \cdot (\frac{\vec{q}}{m_M} \times \vec{S}_\chi)]\frac{\vec{q}}{m_M} \cdot \vec{S}_N$	$-\frac{m_N}{m_\chi}\frac{\vec{q}^2}{m_M^2}\mathcal{O}_{10} - 4\frac{\vec{q}^2}{m_M^2}\mathcal{O}_{12} - 4\frac{m_N^2}{m_M^2}\mathcal{O}_{15}$	O/O
13	$\bar{\chi}\gamma^\mu\gamma^5\chi\bar{N}\gamma_\mu N$	$2\vec{v}^\perp \cdot \vec{S}_\chi + 2i\vec{S}_\chi \cdot (\vec{S}_N \times \frac{\vec{q}}{m_N})$	$2\mathcal{O}_8 + 2\mathcal{O}_9$	O/E
14	$\bar{\chi}\gamma^\mu\gamma^5\chi\bar{N}i\sigma_{\mu\alpha}\frac{q^\alpha}{m_M}N$	$4i\vec{S}_\chi \cdot (\frac{\vec{q}}{m_M} \times \vec{S}_N)$	$-4\frac{m_N}{m_M}\mathcal{O}_9$	O/E
15	$\bar{\chi}\gamma^\mu\gamma^5\chi\bar{N}\gamma^\mu\gamma^5 N$	$-4\vec{S}_\chi \cdot \vec{S}_N$	$-4\mathcal{O}_4$	E/E
16	$i\bar{\chi}\gamma^\mu\gamma^5\chi\bar{N}i\sigma_{\mu\alpha}\frac{q^\alpha}{m_M}\gamma^5 N$	$4i\vec{v}^\perp \cdot \vec{S}_\chi \frac{\vec{q}}{m_M} \cdot \vec{S}_N$	$4\frac{m_N}{m_M}\mathcal{O}_{13}$	E/O
17	$i\bar{\chi}i\sigma^{\mu\nu}\frac{q_\nu}{m_M}\gamma^5\chi\bar{N}\gamma_\mu N$	$2i\frac{\vec{q}}{m_M} \cdot \vec{S}_\chi$	$2\frac{m_N}{m_M}\mathcal{O}_{11}$	O/O
18	$i\bar{\chi}i\sigma^{\mu\nu}\frac{q_\nu}{m_M}\gamma^5\chi\bar{N}i\sigma_{\mu\alpha}\frac{q^\alpha}{m_M}N$	$\frac{\vec{q}}{m_M} \cdot \vec{S}_\chi [i\frac{\vec{q}^2}{m_N m_M} - 4\vec{v}^\perp \cdot (\frac{\vec{q}}{m_M} \times \vec{S}_N)]$	$\frac{\vec{q}^2}{m_M^2}\mathcal{O}_{11} + 4\frac{m_N^2}{m_M^2}\mathcal{O}_{15}$	O/O
19	$i\bar{\chi}i\sigma^{\mu\nu}\frac{q_\nu}{m_M}\gamma^5\chi\bar{N}\gamma_\mu\gamma^5 N$	$-4i\frac{\vec{q}}{m_M} \cdot \vec{S}_\chi \vec{v}^\perp \cdot \vec{S}_N$	$-4\frac{m_N}{m_M}\mathcal{O}_{14}$	E/O
20	$i\bar{\chi}i\sigma^{\mu\nu}\frac{q_\nu}{m_M}\gamma^5\chi\bar{N}i\sigma_{\mu\alpha}\frac{q^\alpha}{m_M}\gamma^5 N$	$4\frac{\vec{q}}{m_M} \cdot \vec{S}_\chi \frac{\vec{q}}{m_M} \cdot \vec{S}_N$	$4\frac{m_N^2}{m_M^2}\mathcal{O}_6$	E/E